



HHS Public Access

Author manuscript

J Proteome Res. Author manuscript; available in PMC 2018 August 04.

Author Manuscript

Author Manuscript

Author Manuscript

Author Manuscript

Published in final edited form as:

J Proteome Res. 2017 August 04; 16(8): 2709–2728. doi:10.1021/acs.jproteome.6b00981.

Proteomics profiling of exosomes from primary mouse osteoblasts under proliferation versus mineralization conditions and characterization of their uptake into prostate cancer cells

Mehmet Asim Bilen^{1,±}, Tianhong Pan², Yu-Chen Lee¹, Song-Chang Lin¹, Guoyu Yu¹, Jing Pan⁴, David Hawke⁵, Bih-Fang Pan⁵, Jody Vykoukal¹, Kavanya Gray¹, Robert L Satcher², Gary E. Gallick³, Li-Yuan Yu-Lee⁴, and Sue-Hwa Lin^{1,3,*}

¹Department of Translational Molecular Pathology, The University of Texas M. D. Anderson Cancer Center, Houston, Texas 77030

²Department of Orthopedic Oncology, The University of Texas M. D. Anderson Cancer Center, Houston, Texas 77030

³Department of Genitourinary Medical Oncology, The University of Texas M. D. Anderson Cancer Center, Houston, Texas 77030

⁴Department of Medicine, Baylor College of Medicine, Houston, Texas 77030

⁵The Proteomics and Metabolomics Facility, The University of Texas M. D. Anderson Cancer Center, Houston, Texas 77030

Abstract

Osteoblasts communicate both with normal cells in the bone marrow, and with tumor cells that metastasized to bone. Here we show that osteoblasts release exosomes, we termed osteosomes, which may be a novel mechanism by which osteoblasts communicate with cells in their environment. We have isolated exosomes from undifferentiated/proliferating (D0 osteosomes) and differentiated/mineralizing (D24 osteosomes) primary mouse calvarial osteoblasts. The D0 and D24 osteosomes were found to be vesicles of 130–140 nm by dynamic light scattering analysis. Proteomics profiling using tandem mass spectrometry (LC-MS/MS) identified 206 proteins in D0 osteosomes and 336 in D24 osteosomes. The proteins in osteosomes are mainly derived from the cytoplasm (~47%) and plasma membrane (~31%). About 69% of proteins in osteosomes are also found in Vesiclepedia, and these canonical exosomal proteins include tetraspanins and Rab family proteins. We found that there are differences in both protein content and levels in exosomes isolated from undifferentiated and differentiated osteoblasts. Among the proteins that are unique to osteosomes, 169 proteins are present in both D0 and D24 osteosomes, 37 are unique to D0, and 167 are unique to D24. Among those 169 proteins present in both D0 and D24 osteosomes, 10

*Correspondence: Dr. Sue-Hwa Lin, Department of Translational Molecular Pathology, The University of Texas M. D. Anderson Cancer Center, 1515 Holcombe Blvd., Houston, TX 77030. slin@mdanderson.org, Tel: 713-794-1559.

±Current address: Department of Hematology and Medical Oncology, Winship Cancer Institute of Emory University, Atlanta, GA, USA

SUPPORTING INFORMATION:

The following files are available free of charge at ACS website <http://pubs.acs.org>:

3) Annotated tandem mass spectra for proteins identified on the basis of a single peptide assignment that are unique in D0 and in D24 osteosomes.

proteins are likely present at higher levels in D24 than D0 osteosomes, based on emPAI ratios of more than 5. These results suggest that osteosomes released from different cellular state of osteoblasts may mediate distinct functions. Using live-cell imaging, we measured the uptake of PKH26-labeled osteosomes into C4-2B4 and PC3-mm2 prostate cancer cells. In addition, we showed that cadherin-11, a cell adhesion molecule, plays a role in the uptake of osteosomes into PC3-mm2 cells as osteosome uptake was delayed by neutralizing antibody against cadherin-11. Together, our studies suggest that osteosomes could have a unique role in the bone microenvironment under both physiological and pathological conditions.

Keywords

osteoblasts; exosomes; osteosomes; cadherin-11; mass spectrometry

Introduction

Under normal physiologic conditions, osteoblasts are in communication with cells in the bone marrow to maintain tissue homeostasis. Osteoblasts have been shown to be a component of hematopoietic stem cell niche^{1–3}, in which cell-cell contact between osteoblast and hematopoietic stem cells leads to Notch activation, which is one mechanism of communication by which osteoblasts influence stem cell function¹. Osteoblasts were also shown to use the paracrine factor, BMP, to regulate hematopoietic stem cells². In pathological conditions, e.g., prostate cancer bone metastasis, osteoblasts and tumor cell communication through paracrine factors have been shown to increase the tumor growth^{4–8}. Osteoblast secreted factors have also been shown to confer tumor cell survival, resulting in resistance to therapy⁹. The unique roles of osteoblasts in the bone microenvironment in both physiological and pathological conditions suggest that the methods of communication between these cell types needs to be fully understood.

In this report, we examined whether exosomes could be an additional mechanism for osteoblast communication with other cells in the bone marrow. Exosomes are extracellular vesicles that originate by the fusion of multivesicular endosomes with the plasma membrane¹⁰. Exosomes are endocytic vesicles released by cells and are enriched in specific proteins, lipids and RNAs, indicating the existence of specialized mechanisms that control the sorting of molecules into exosomes¹¹. Recent discoveries that exosomes are a powerful way of cell-cell communication^{11–17} suggested new possibilities that osteoblasts may use exosomes to bring proteins and genetic modifiers, e.g. miRNAs, into target cells to modulate cell activities. For example, exosomes that are derived from breast cancer stroma have been shown to increase cell migration¹⁸ and confer therapy resistance¹⁹, suggesting a role of stromal exosomes in modulating cancer progression.

One of the unique properties of osteoblasts is their ability to undergo differentiation to form mineralized bone. Whether these differentiation-induced cellular changes may affect exosome composition and thus exosome-mediated intercellular communication remains to be determined. Recently, Ge et al.²⁰ reported the proteomic analysis of microvesicles isolated from nonmineralized mouse MCT3T-E1 cells, a T-antigen immortalized mouse

Author Manuscript
Author Manuscript
Author Manuscript
Author Manuscript

calvarial osteoblast cell line. They showed that the MC3T3-E1 exosomes contained typical exosomal markers, including TSG101 and Flot 1²⁰. Morhayim et al.²¹ reported the proteomic signature of extracellular vesicle (EV) from nonmineralizing and mineralizing T-antigen immortalized human osteoblasts SV-HFO. Among the proteins identified, they detected 3 and 22 osteoblast-specific proteins that were uniquely present in nonmineralizing and mineralizing osteoblasts, respectively²¹.

Exosomes from primary mouse osteoblasts have never been studied. It is known that primary mouse osteoblasts can be induced to differentiate more extensively than immortalized osteoblasts under differentiation conditions, which may more closely reflect normal osteoblast physiology. In this study, we isolated exosomes, which we termed osteosomes, from both undifferentiated/proliferating and differentiated/mineralizing primary mouse osteoblasts and determined the proteomics profile of these osteoblast-derived exosomes. Our study showed that the molecular compositions of osteosomes under undifferentiated and differentiated conditions are different, with 225 proteins uniquely present in osteosomes from differentiated but not undifferentiated osteoblasts. We also showed that cadherin-11 cell adhesion molecules play a role in the uptake of osteosomes into prostate cancer cells.

Experimental Section

Exosome-depleted FBS preparation

To deplete exosomes in serum, fetal bovine serum (FBS) was mixed with 50% polyethylene glycol (Fluka, polyethylene glycol 10,000) at 5:1 ratio. After incubation at 4°C for 2h, solution was centrifuged at 1,500g for 30 minutes at 4°C. Supernatant was collected and used as exosome-depleted FBS.

Osteoblast isolation and differentiation

Calvaria were isolated from 2–3 day old newborn mice. Collected bone tissue was twice digested using 0.1mg/mL collagenase in alpha-MEM with 1:40 diluted trypsin. These first two digestions were discarded and a third digestion using 0.2 mg/mL collagenase was performed and osteoblasts were collected. Along with undigested bone, osteoblasts were transferred to cell culture plates and allowed to grow to confluence with minimal disturbance for three days. Cell and bone fragments were trypsinized, washed, and passaged in fresh media containing exosome-depleted FBS. Cells were allowed to grow to confluence and conditioned media was collected (D0 conditioned media). The media was changed to differentiation media containing 10% exosome-depleted FBS, 5mM beta-glycerophosphate, and 100ug/mL ascorbic acid. Differentiation media was replenished every three days for a total of 24 days. At day 24, cell media was collected (D24 conditioned media).

Osteoblast differentiation assays

Von Kossa staining for mineralized bone matrix was performed as described elsewhere²². Alizarin Red S staining for calcium deposition was carried out as below: 2 g Alizarin Red S (C. I. 58005) was dissolved in 100 ml distilled water, and pH was adjusted to 4.1 – 4.3 with 0.1% NH4OH to prepare the Alizarin Red S staining solution. Filter the dark-brown solution and store it in the dark. The cell was taken from the incubator and the medium was carefully

aspirated. Then the cells were washed with Dulbecco's PBS, without $\text{Ca}^{2+}/\text{Mg}^{2+}$. For fixation, the neutral buffered formalin (10%) was used to cover the cellular monolayer and incubate at least 30 min. Then the formalin was carefully aspirated and the cells were washed with distilled water. Then enough Alizarin Red S staining solution was added to cover the cellular monolayer and incubated at room temperature in the dark for 45 min. Then the Alizarin Red S staining solution was carefully aspirated and was washed four times with 1 ml distilled water. Then PBS was added to cover the cellular monolayer and analyzed in light microscopy.

Reverse transcription and real-time PCR (qRT-PCR)

RNA was prepared using Trizol (InVitrogen) and further purified by RNAeasy mini kit plus DNase I treatment (Qiagen). The relative mRNA level for each gene was quantified by Real-time RT-PCR with SYBR Green (Applied Biosystems), using *Gapdh* as a control. The primers for RT-PCR are as follow. Alkaline phosphatase: CTCCTCCATCCCCTCCCTTC and CCCTGGGTAGACAGCCAAC; osteocalcin: GCTCTGTCTCTGACCTCA and TGGACATGAAGGCTTGTC; DMP1: CCCACGAACAGTGAGTCATC and GGTCTGTACTGGCCTCTGTC; SOST: ATCCCAGGGCTTGGAGAGTA and CTCGGACACATCTTGGCGT; GAPDH: CCCAGAAGACTGTGGATG and GCAGGGATGATGTTCTGG.

Exosome isolation and analysis

Osteoblasts were isolated from 80 newborn mouse calvaria and grew to confluence in exosome-depleted fetal bovine serum. The conditioned medium was collected and centrifuged at 1000×g for 5 min to remove cells, followed by an initial filtration step (1 μm) and a centrifugation step of 3000×g for 10 min to remove cellular debris. A total of 150 ml of conditioned medium was collected and ultracentrifuged at 100,000×g at 4°C overnight. The exosome pellet from the ultracentrifugation step was resuspended in 10 ml of PBS and a second step of ultracentrifugation was performed at 100,000×g at 4°C for 2 h. The pellet was resuspended in PBS and ultracentrifuged at 100,000×g one more time to remove fetal bovine serum. Osteosomes were isolated from day 0-CM and day 24-CM by serial centrifugation. In brief, media was centrifuged at 2,000g for 20 min, supernatant was then centrifuged again at 10,000g for 30 min. Supernatant was again collected and spun at 100,000g for 90 min, exosome pellet collected, washed with 1× PBS and spun at 100,000g for 90 min. Supernatant was discarded and pellet was resuspended in 1×PBS for further analysis.

Exosome particle size determination and transmission electron microscopy

The particle sizes of isolated D0 and D24 exosomes were measured by dynamic light scattering analysis using NanoSight LM-10 instrument (Nanosight Limited, Amesbury, UK). Transmission electron microscopy (TEM) was performed by MD Anderson Core facility. Samples were fix in the final concentration of 2% glutaraldehyde and were placed on 100 mesh carbon coated, formvar coated copper grids treated with poly-L-lysine for 1 hour. Samples were then negatively stained with Millipore-filtered aqueous 1% uranyl acetate for 1 min. Stain was blotted dry from the grids with filter paper and samples were allowed to dry. Samples were then examined in a JEM 1010 transmission electron microscope (JEOL,

USA, Inc., Peabody, MA) at an accelerating voltage of 80 Kv. Digital images were obtained using the AMT Imaging System (Advanced Microscopy Techniques Corp., Danvers, MA).

Proteomics profiling

The osteosome were acetone precipitated (acetone:sample=5:1 ratio) and placed in -20°C overnight. The precipitated proteins were resuspended in 10 µl Rapigest (2 mg/ml in 100 mM ammonium bicarbonate) (Waters) plus 30 µl 50 mM ammonium bicarbonate, heated at 100°C for 10 min. The samples were cooled to room temperature and digested with 200–400 ng sequencing grade trypsin (20 ng/µl in 0.02% formic acid) (Promega) at 37°C overnight. The digested samples were dried down using Speedvac and reconstitute in 1% formic acid.

The resulting peptides were analyzed by liquid chromatography-tandem mass spectrometry (LC-MS/MS) on an Orbitrap Fusion mass spectrometer (Thermo Scientific). HPLC analyses were performed with Dionex RSCL 3000 Nano. Samples were injected into a Phenomenex core-shell C18 DB column (2.7 µm 15cm), with mobile phase compositions of A: 0.1% formic acid in water, B: 0.1% formic acid in acetonitrile and with a flow rate of 100. The gradient was held isocratic at 2% B for 2 min, ramped up to 35% at 165 min, ramped up to 80% at 166 min, maintained at 80% until 176 min, ramped down to 2% at 177 min, held at 2% until 190 min.

MS parameters and scan strategy were: (a) mass range for MS1: 400–1300; (b) mass resolution for MS1: 500,000; (c) mass window for precursor ion selection: 0.5d; (d) number or precursors selected for tandem MS in each scan cycle: Maximum in 2 sec; (e) mass analyzer for tandem-MS: MS1: Orbitrap; MS2: Iontrap. (f) charge state screening parameters: 2-4; (g) relative collision energy: 30%; (h) dynamic exclusion settings: 15sec.

Data processing of the MS results were as follows: (a) Database: SwissProt/2.3.02, SwissProt_040115.fasta, Total sequences: 548208; (b) Search engine: Mascot 2.5 via Proteome Discoverer 1.4; (c) Precursor and product ion mass tolerances: Peptide Mass Tolerance: 10, Peptide Mass Tolerance Units: ppm, Fragment Mass Tolerance: 0.8, Fragment Mass Tolerance Units: Da, Ions score cut-off: 20; (d) Enzyme specificity: Trypsin, 2 missed cleavages allowed; (e) Fixed and variable modifications: Fixed: none, Variable modifications: Oxidation (M), Gln->pyro-Glu (N-term Q), Trioxidation (C); (f) Additional search specifications: Decoy database also searched; (g) Method for FDR assessment: Decoy DB using Proteome Discoverer; (h) Criteria for acceptance of peptide assignments and protein identifications: Significance threshold: 0.05. Max. number of hits: auto. Use MudPIT protein scoring: not applicable; (i) Determination of probability of modification site location: not applicable.

Immunoblot

Proteins from osteosomes were subjected to 4–12% sodium dodecyl sulfate–polyacrylamide gel electrophoresis. The gel was transferred to a nitrocellulose membrane (Schleicher & Schnell) and stained with Ponceau S, followed by immunoblotting with specific antibodies as indicated. Signals were detected with a chemiluminescent detection kit (Pierce Biotechnology).

Exosome uptake and antibody blocking

Osteosomes and control liposomes were labeled with the red fluorescent lipophilic dye PKH26 (InVitrogen)²³. Next, PKH26-labeled osteosomes or liposomes (3×10^5 particles) were added to prostate cancer cells (1×10^4 cells), C4-2b or PC3-mm2, in RPMI1640 containing exosome-depleted 0.1% FBS, and cells were plated on a glass-bottom dish (ibidi). Exosome or liposome uptake into cells was observed by live-cell imaging on a BioStation (Nikon), in which images were captured every 30 min over 30 h using both bright-field and red fluorescence channels²⁴. For antibody blocking, PKH26-labeled osteosomes were preincubated with anti-Cad11 monoclonal antibody 1A5²⁵ at a final antibody concentration of 3 µg/ml before the osteosome-antibody mixture was added to prostate cancer cells for live-cell imaging analysis. PBS buffer alone and an unrelated antibody with similar IgG isotype were used as negative controls.

Results

Undifferentiated (D0) and Differentiated (D24) osteoblasts

Osteoblasts can be stimulated to undergo proliferation or differentiation, depending on the specific treatments or culture condition. It is not clear whether exosomes generated from undifferentiated or differentiated osteoblasts have different protein composition. To address this question, performed proteomics profiling of exosomes, which we term osteosomes, from undifferentiated or differentiated osteoblasts. The experimental scheme for the isolation and characterization of exosomes from primary mouse osteoblasts is shown in Fig. 1A.

Osteoblasts isolated from newborn calvaria were cultured in the growth medium to confluence (undifferentiating condition) and the medium was then changed to differentiation medium and the osteoblasts further cultured for 24 days (differentiating condition). The morphologies of osteoblasts cultured in undifferentiating condition (D0 osteoblasts) and differentiating condition (D24 osteoblasts) are shown in Fig. 1B. Von Kossa (Fig. 1C) and alizarin staining (Fig. 1D) showed that D24 but not D0 osteoblasts are mineralized. qRT-PCR for the expression of markers of osteoblast differentiation in mRNA prepared from D0 and D24 osteoblasts was used to establish the differentiation status of osteoblasts. In one experiment, alkaline phosphatase and osteocalcin, markers of osteoblast differentiation, were increased by 20- and 2876-fold, respectively in Day 24 osteoblasts compared to D0 osteoblasts (Fig. 1E). In another experiment, the increases were 17- and 242-fold, respectively (Supplemental –Fig. S1). In addition, the osteocyte markers, dentin matrix acidic phosphoprotein 1 (DMP1) and sclerostin (SOST1), were also increased by 730- to 1076-fold and 1537- to 91,650-fold, respectively, in D24 osteoblasts compared to D0 osteoblasts (Fig. 1E, Supplemental Fig. S1). These results confirm that these osteoblasts have undergone differentiation after culturing in the differentiation medium for 24 days.

Characterization of osteosomes isolated from D0 and D24 osteoblasts

Conditioned media were collected from D0 and D24 osteoblasts and exosomes were isolated using ultracentrifugation. Exosomes prepared from the undifferentiated (D0 osteoblasts) and differentiated (D24 osteoblasts) conditions are named D0 and D24 osteosomes, respectively. When examined by light scattering spectroscopy, both D0 and D24 osteosomes have particle sizes around 100 nm (Fig. 2A, C), which is the typical size of exosomes. Transmission

Author Manuscript
Author Manuscript
Author Manuscript
Author Manuscript

electron microscopy (TEM) showed that both the osteosome vesicles (D0 and D24) exhibit a cup-shaped morphology (Fig. 2B, 2D), which is the characteristic morphology of exosomes. The average sizes of D0 and D24 osteosomes from four independent experiments were 134.9 ± 12.6 and 138.9 ± 12.5 , respectively (Fig 2E). We note that the number of osteosomes from primary mouse osteoblasts is very low, ~ 4000 and ~3300 particles per million cells from undifferentiated and differentiated osteoblasts, respectively. In contrast, the exosomes from C4-2B4 and PC3-mm2 PCa cells are ~184,000 and 108,000 particles per million cells. Thus, the number of exosomes from primary mouse osteoblasts is around 2–4% of those from PCa cells.

Comparison of osteosomal proteins with other exosomal proteins

To characterize the proteins in osteosomes, D0 and D24 osteosomes were subjected to mass spectrometry analysis. Proteomics profiling by mass spectrometry identified 206 and 336 proteins with a 1% false discovery rate (FDR) from D0 and D24 osteosomes, respectively (Fig. 3A). 169 proteins were found in both D0 and D24 osteosomes, resulting in a total of 373 osteosomal proteins from combining the proteins from D0 and D24 osteosomes. A comparison of our osteosome proteomics data with a published exosome database, i.e., Vesiclepedia²⁶, showed that 256 (69%) proteins are also found in Vesiclepedia (Fig. 3B), resulting in 117 proteins that are unique to osteosomes. The canonical exosome proteins¹⁰ found in osteosomes are shown in Supplemental Table S1. They include tetraspanins (CD9, CD81), endosomal molecules (clathrin), multivesicular body proteins (Chmp4b), membrane trafficking proteins (RAB proteins, annexins), cytoskeletal proteins (actin, tubulin, myosin), heat shock proteins (HSP90, HSP70), and adhesion proteins (integrins). The molecular composition of osteosomes reflects their origin in endosomes. These results demonstrate that osteosomes have similar characteristics as exosomes from other cell types.

Ingenuity pathway analysis of osteosomal proteins

Analysis of the 373 osteosomal proteins from combining the proteins from D0 and D24 osteosomes using Ingenuity Pathway Analysis showed that the osteosomal proteins are originated from the cytoplasm (47%) and plasma membrane (31%) (Fig. 3C). We further analyzed these proteins based on the potential biological processes and found that these proteins are involved in integrin signaling, RhoGDI, and remodeling of epithelial adherens junctions (Fig. 3D). Importantly, the disease function analysis showed that these osteosome proteins are mainly involved in cell movement, cell death and survival, cellular assembly and cancer (Fig. 3E).

Changes in the levels of osteosomal proteins during osteoblast differentiation

Among the 117 proteins that are unique to osteosomes (Fig. 4A), 30 proteins are common between D0 and D24 osteosomes (Table 1). This results in 11 proteins that are unique to D0 osteosomes (Fig. 4A, Table 2) and 76 proteins that are unique to D24 osteosomes (Fig. 4A, Table 3). For the 169 proteins that are common between D0 and D24 osteosomes, we compared their levels of expression under different differentiation status. Although the mass spectrometry method we used for protein identification is not quantitative, the Experimentally Modified Protein Abundance Index (emPAI) can provide an estimate for the relative levels of expression. A comparison of emPAI scores among the 169 common

osteosome proteins, 10 of the 169 proteins (6%) show a greater than 5-fold increase in D24 osteosomes when compared to D0 osteosomes (Fig. 4B). Among them, the protein with the highest fold of increase is alkaline phosphatase (ALPL, 15-fold). When protein scores were used as comparison, seven of these proteins also have more than 5-fold increase (Fig. 4C). Measurement of the enzymatic activity of alkaline phosphatase in D0 and D24 osteosomes showed that there was an increase, about 3.5-fold, in D24 osteosomes compared to that in D0 osteosomes (Fig. 4D), confirming the results from mass spectrometry analysis. These observations suggest that osteosome compositions differ depending on the differentiation states of osteoblasts.

Osteosome proteins that mediate osteosome uptake into prostate cancer cells

Uptake of exosomes has been shown to be the mechanism by which exosomes modulate their target cells. It has been reported that vesicle targeting depends on the type and activation status of recipient cells^{27, 28}. To assess if prostate cancer cells take up released osteosomes, we investigated the uptake of osteosomes by different prostate cancer cell lines. Osteosomes or control liposomes were labeled with PKH26 dye. PKH26-labeled osteosomes or control liposomes were then co-cultured with C4-2b prostate cancer cells for various times and monitored by live-cell imaging to detect the time course of osteosome transfer into C4-2b cells. We observed an increase in osteosome uptake in C4-2b cells, with close to 60% of cells showing osteosome uptake by 10 h and 100% by 30 h (Fig. 5A). In contrast, during the same time frame, little uptake of control liposomes was detected in C4-2b cells at 10 h, and only ~20% C4-2b cells took up liposomes by 30 h. In PC3-mm2 cells, more than 60% of cells showed osteosome uptake by 10 h and 100% by 30 h (Fig. 5B). In contrast, uptake of control liposomes in PC3-mm2 cells was very low at 10 h, reaching ~50% by 30 h. The results using two different prostate cancer cell lines show that prostate cancer cells take up osteosomes more readily than control liposomes. These findings raise the possibility that osteosomes may contain cell surface molecules that facilitate their uptake into PCa cells.

Cad11 contributes to the uptake of osteosomes into PC3-mm2 cells

We next examined whether osteosomes may contain specific membrane proteins that facilitate interaction with PC3-mm2 cells through cell surface adhesion molecules and/or receptors to favor their capture by PC3-mm2 cells. Our previous studies have shown that the osteoblast cadherin, cadherin11 (Cad11, also known as OB-cadherin) plays a role in the homing of PC3-mm2 cells, which express Cad11, to bone through interacting with Cad11 expressed on osteoblasts^{25, 29}. We found that Cad 11 is a common osteosomal protein in both D0 and D24 osteosomes (Table 1). Cad11 is a homophilic cell adhesion molecule. Thus, Cad11 on osteosomes may enhance the uptake of osteosomes into PC3-mm2 cells through interaction with Cad11 on PC3-mm2 cells. The emPAI values of Cad11 in D0 vs D24 osteosomes were 0.06 and 0.11, respectively, and the mascot score were 30 and 54, respectively (Table 1). Western blot for the levels of Cad11 in osteosomes showed that the level of Cad11 were similar, although D24 seemed to be slightly lower when compared to D0 osteosomes (Fig. 5C).

To examine the role of Cad11 in osteosome uptake into PC3-mm2 cells, we used a Cad11 adhesion-blocking antibody mAb1A5²⁵ in live-cell imaging analysis. PKH26-labeled

osteosomes were preincubated for 30 min with Cad11 mAb1A5, a control antibody with matching isotype (IgG) or buffer alone, and the antibody-osteosome mixture was added to PC3-mm2 cells at a final concentration of 3 μ g/ml mAb. As shown in Fig. 5D, the control cells treated with either buffer alone or an irrelevant mAb showed a similar time course of osteosome uptake, with about 50% of PC3-mm2 cells positive with osteosomes at 5 h. Treatment of osteosomes with Cad11 mAb 1A5 delayed osteosome uptake into PC3-mm2 cells, with 50% cell uptake reached at 9 h. These results suggest that Cad11 contributes to the uptake of osteosomes into PC3-mm2 cells, likely mediated through homophilic Cad11 adhesion interactions. We note that C4-2b cells do not express detectable levels of Cad11²⁹, yet osteosomes can still be efficiently taken up relative to liposomes (Fig. 5A), suggesting that interactions of other membrane components between osteosomes and C4-2b cells likely mediate osteosome uptake into C4-2b cells. Together, these observations suggest that osteosome uptake is dependent on the expression of cell surface adhesion molecules, and that diverse membrane components of different PCa cells might be involved in osteosome uptake into different PCa cells.

Discussion

We have identified a unique set of proteins in exosomes derived from primary mouse osteoblasts termed “osteosomes”. In addition, we showed that there are significant differences in the levels and content of proteins in osteosomes isolated from undifferentiated versus differentiated osteoblasts, with 167 proteins uniquely present in osteosomes from differentiated but not undifferentiated osteoblasts. Our studies expand the list of exosome proteins differentially expressed in mineralized osteoblasts and suggest that osteosomes may mediate different functions depending on their cellular state. Furthermore, we showed that the adhesion molecules, such as cadherin-11, on the osteosome surface play a role in osteosome uptake into PCa cells. As PC3-mm2 is a highly metastatic PCa cell line, it is possible that uptake of osteosomes through cadherin-11 contributes to the metastatic potential of PC3-mm2 cells. This is the first report on the isolation and proteomics profiling of exosomes from primary mouse osteoblasts. Our study offers an additional mechanism, besides cell-cell contact and paracrine factors, by which osteoblasts may be used to communicate with cells in the bone marrow microenvironment in both physiological and pathological conditions.

The low number of osteosomes from primary mouse osteoblasts has limited our ability to examine the functional roles of osteosomes on PCa cells. Despite these challenges, our studies raise the possibility that osteosomes play a role in modulating the activities of tumor cells that have metastasized to bone. Exosomes derived from tumor-associated stroma have been shown to increase tumor cell migration through Wnt-PCP signaling¹⁸, and stromal exosomes have been shown to confer therapy resistance to breast cancer cells¹⁹. PCa is a unique malignancy with a special affinity for the bone and a remarkable capacity to develop osteoblastic metastasis⁴. We recently demonstrated that PCa-induced aberrant bone overgrowth promotes tumor growth in bone⁷. While factors secreted from osteoblasts, such as osteonectin, osteopontin, osteocalcin and bone sialoprotein, have been shown to affect different PCa cell functions^{30–33}, a role of osteosomes in PCa progression in bone has never been studied. Morhayim et al.²¹ showed that upon incubating the extracellular vesicles,

isolated from differentiated osteoblastic cell line SV-immortalized human osteoblasts, with PC3 PCa cells, a 2-fold increase in cell growth compare to medium control was observed. Whether such an effect also occurs *in vivo* awaits further studies.

Exosomes contain specific repertoires of proteins as well as RNAs, indicating the existence of mechanisms that control the sorting of molecules into exosomes. During osteoblast differentiation, there is a significant change in the expression of proteins, as reflected in the dramatic increases in osteoblast differentiation markers alkaline phosphatase, osteocalcin, DMP1 and sclerostin (Fig. 1E). Among the osteoblast differentiation markers examined, only alkaline phosphatase was found in D24 osteoblasts. In addition, the differentiation status of osteoblasts also affects the composition of exosomes. We found that several proteins are uniquely present in D24 but not D0 osteosomes. How proteins and RNAs are selected and sorted into exosomes is not clear³⁴. The differential expression of proteins, and likely RNAs, between D0 and D24 osteosomes will likely affect the outcome of the communication between the osteoblasts (exosome-producer) and the recipient cells. This issue is under intense investigation. Isolation of osteosomes and the identification of components in osteosomes opened new possibilities that osteoblasts may use osteosomes to modulate cells in the bone marrow. Previous studies by Calvi et al.¹ and Zhang et al.² showed that osteoblasts regulate hematopoietic stem cell activity through cell-cell contact, leading to Notch activation and paracrine BMP signaling, respectively. It is intriguing to consider that osteosomes may be an additional mechanism by which osteoblasts regulate hematopoietic stem cells. Because osteosomes can bring genetic modifiers, in addition to proteins, to hematopoietic stem cells, osteosomes may represent a novel mechanism to regulate hematopoiesis. Further studies on the osteosome RNA contents and their effects on resident bone marrow cells and metastatic cancer cells are warranted.

Conclusions

Our studies suggest that osteosomes may play a role in the interaction between osteoblasts and cells in the bone marrow microenvironment in both physiological and pathological conditions.

Supplementary Material

Refer to Web version on PubMed Central for supplementary material.

Acknowledgments

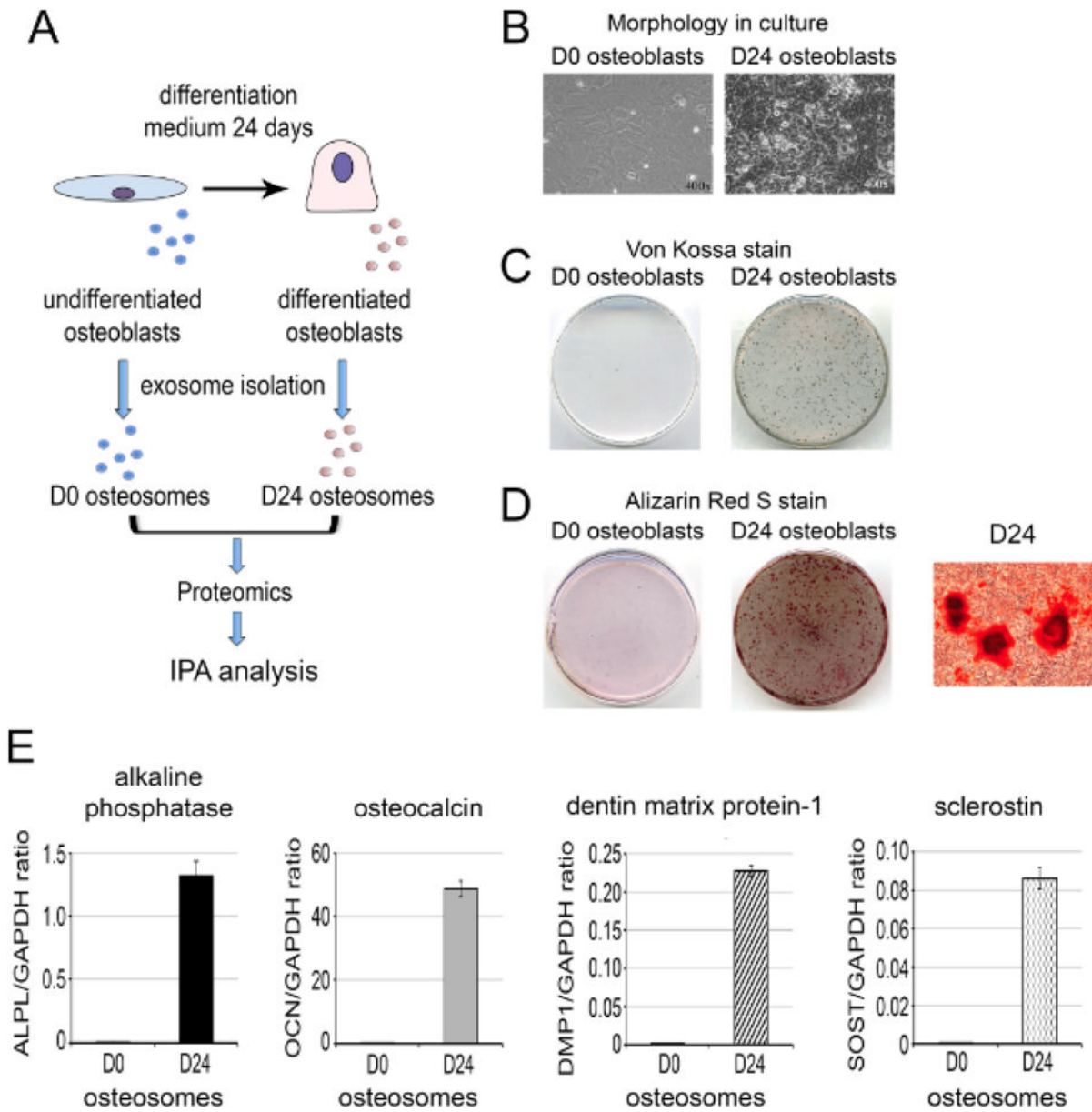
This work was supported by grants from the NIH including CA174798, 5P50 CA140388 and P30CA16672, the Prostate Cancer Foundation, Cancer Prevention and Research Institute of Texas (CPRIT RP110327, CPRIT RP150179, CPRIT RP150282), funds from the University Cancer Foundation via the Sister Institute Network Fund at the MD Anderson Cancer Center.

References

1. Calvi LM, Adams GB, Weibreht KW, Weber JM, Olson DP, Knight MC, Martin RP, Schipani E, Divieti P, Bringhurst FR, Milner LA, Kronenberg HM, Scadden DT. Osteoblastic cells regulate the haematopoietic stem cell niche. *Nature*. 2003; 425(6960):841–6. [PubMed: 14574413]

2. Zhang J, Niu C, Ye L, Huang H, He X, Tong WG, Ross J, Haug J, Johnson T, Feng JQ, Harris S, Wiedemann LM, Mishina Y, Li L. Identification of the haematopoietic stem cell niche and control of the niche size. *Nature*. 2003; 425(6960):836–41. [PubMed: 14574412]
3. Coskun S, Chao H, Vasavada H, Heydari K, Gonzales N, Zhou X, de Crombrugghe B, Hirschi KK. Development of the fetal bone marrow niche and regulation of HSC quiescence and homing ability by emerging osteolineage cells. *Cell Rep*. 2014; 9(2):581–90. [PubMed: 25310984]
4. Logothetis C, Lin S-H. Osteoblasts in prostate cancer metastasis to bone. *Nature Reviews Cancer*. 2005; 5:21–28. [PubMed: 15630412]
5. Dai J, Keller J, Zhang J, Lu Y, Yao Z, Keller ET. Bone morphogenetic protein-6 promotes osteoblastic prostate cancer bone metastases through a dual mechanism. *Cancer Res*. 2005; 65:8274–85. [PubMed: 16166304]
6. Dai J, Kitagawa Y, Zhang J, Yao Z, Mizokami A, Cheng S, Nor J, McCauley LK, Taichman RS, Keller ET. Vascular endothelial growth factor contributes to the prostate cancer-induced osteoblast differentiation mediated by bone morphogenetic protein. *Cancer Res*. 2004; 64:994–999. [PubMed: 14871830]
7. Lee YC, Cheng CJ, Bilen MA, Lu JF, Satcher RL, Yu-Lee LY, Gallick GE, Maity SN, Lin SH. BMP4 promotes prostate tumor growth in bone through osteogenesis. *Cancer Res*. 2011; 71(15): 5194–203. [PubMed: 21670081]
8. Li Y, Sikes RA, Malaeb BS, Yeung F, Law A, Graham SE, Pei M, Kao C, Nelson J, Koeneman KS, Chung LW. Osteoblasts can stimulate prostate cancer growth and transcriptionally down-regulate PSA expression in cell line models. *Urol Oncol*. 2011; 29(6):802–8. [PubMed: 20451417]
9. Lee YC, Lin SC, Yu G, Cheng CJ, Liu B, Liu HC, Hawke DH, Parikh NU, Varkaris A, Corn P, Logothetis C, Satcher RL, Yu-Lee LY, Gallick GE, Lin SH. Identification of Bone-Derived Factors Conferring De Novo Therapeutic Resistance in Metastatic Prostate Cancer. *Cancer Res*. 2015; 75(22):4949–59. [PubMed: 26530902]
10. Thery C, Zitvogel L, Amigorena S. Exosomes: composition, biogenesis and function. *Nat Rev Immunol*. 2002; 2(8):569–79. [PubMed: 12154376]
11. Lakkaraju A, Rodriguez-Boulan E. Itinerant exosomes: emerging roles in cell and tissue polarity. *Trends Cell Biol*. 2008; 18(5):199–209. [PubMed: 18396047]
12. Thery C, Ostrowski M, Segura E. Membrane vesicles as conveyors of immune responses. *Nat Rev Immunol*. 2009; 9(8):581–93. [PubMed: 19498381]
13. Mittelbrunn M, Sanchez-Madrid F. Intercellular communication: diverse structures for exchange of genetic information. *Nat Rev Mol Cell Biol*. 2012; 13(5):328–35. [PubMed: 22510790]
14. Valadi H, Ekstrom K, Bossios A, Sjstrand M, Lee JJ, Lotvall JO. Exosome-mediated transfer of mRNAs and microRNAs is a novel mechanism of genetic exchange between cells. *Nat Cell Biol*. 2007; 9(6):654–9. [PubMed: 17486113]
15. Fevrier B, Raposo G. Exosomes: endosomal-derived vesicles shipping extracellular messages. *Curr Opin Cell Biol*. 2004; 16(4):415–21. [PubMed: 15261674]
16. Nieuwland R, Sturk A. Why do cells release vesicles? *Thromb Res*. 2010; 125(Suppl 1):S49–51. [PubMed: 20149923]
17. Mathivanan S, Ji H, Simpson RJ. Exosomes: extracellular organelles important in intercellular communication. *J Proteomics*. 2010; 73(10):1907–20. [PubMed: 20601276]
18. Luga V, Zhang L, Viloria-Petit AM, Ogunjimi AA, Inanlou MR, Chiu E, Buchanan M, Hosein AN, Basik M, Wrana JL. Exosomes mediate stromal mobilization of autocrine Wnt-PCP signaling in breast cancer cell migration. *Cell*. 2012; 151(7):1542–56. [PubMed: 23260141]
19. Boelens MC, Wu TJ, Nabey BY, Xu B, Qiu Y, Yoon T, Azzam DJ, Twyman-Saint Victor C, Wiemann BZ, Ishwaran H, Ter Brugge PJ, Jonkers J, Slingerland J, Minn AJ. Exosome transfer from stromal to breast cancer cells regulates therapy resistance pathways. *Cell*. 2014; 159(3):499–513. [PubMed: 25417103]
20. Ge M, Ke R, Cai T, Yang J, Mu X. Identification and proteomic analysis of osteoblast-derived exosomes. *Biochem Biophys Res Commun*. 2015; 467(1):27–32. [PubMed: 26420226]
21. Morhayim J, van de Peppel J, Demmers JA, Kocer G, Nigg AL, van Driel M, Chiba H, van Leeuwen JP. Proteomic signatures of extracellular vesicles secreted by nonmineralizing and

- mineralizing human osteoblasts and stimulation of tumor cell growth. *FASEB J.* 2015; 29(1):274–85. [PubMed: 25359493]
22. Bhargava U, Bar-Lev M, Bellows CG, Aubin JE. Ultrastructural analysis of bone nodules formed in vitro by isolated fetal rat calvaria cells. *Bone.* 1988; 9:155–163. [PubMed: 3166832]
23. Medina A, Ghahary A. Transdifferentiated circulating monocytes release exosomes containing 14-3-3 proteins with matrix metalloproteinase-1 stimulating effect for dermal fibroblasts. *Wound Repair Regen.* 2010; 18(2):245–53. [PubMed: 20409149]
24. Deeraksa A, Pan J, Sha Y, Liu XD, Eissa NT, Lin SH, Yu-Lee LY. Plk1 is upregulated in androgen-insensitive prostate cancer cells and its inhibition leads to necroptosis. *Oncogene.* 2013; 32(24): 2973–83. [PubMed: 22890325]
25. Lee YC, Bilen MA, Yu G, Lin SC, Huang CF, Ortiz A, Cho H, Song JH, Satcher RL, Kuang J, Gallick GE, Yu-Lee LY, Huang W, Lin SH. Inhibition of cell adhesion by a cadherin-11 antibody thwarts bone metastasis. *Mol Cancer Res.* 2013; 11(11):1401–11. [PubMed: 23913163]
26. Kalra H, Simpson RJ, Ji H, Aikawa E, Altevogt P, Askenase P, Bond VC, Borras FE, Breakefield X, Budnik V, Buzas E, Camussi G, Clayton A, Cocucci E, Falcon-Perez JM, Gabrielsson S, Gho YS, Gupta D, Harsha HC, Hendrix A, Hill AF, Inal JM, Jenster G, Kramer-Albers EM, Lim SK, Llorente A, Lotvall J, Marcilla A, Mincheva-Nilsson L, Nazarenko I, Nieuwland R, Nolte-'t Hoen EN, Pandey A, Patel T, Piper MG, Pluchino S, Prasad TS, Rajendran L, Raposo G, Record M, Reid GE, Sanchez-Madrid F, Schiffelers RM, Siljander P, Stensballe A, Stoorvogel W, Taylor D, Thery C, Valadi H, van Balkom BW, Vazquez J, Vidal M, Wauben MH, Yanez-Mo M, Zoeller M, Mathivanan S. Vesiclepedia: a compendium for extracellular vesicles with continuous community annotation. *PLoS Biol.* 2012; 10(12):e1001450. [PubMed: 23271954]
27. Segura E, Guerin C, Hogg N, Amigorena S, Thery C. CD8+ dendritic cells use LFA-1 to capture MHC-peptide complexes from exosomes in vivo. *J Immunol.* 2007; 179(3):1489–96. [PubMed: 17641014]
28. Nolte-'t Hoen EN, Buschow SI, Anderton SM, Stoorvogel W, Wauben MH. Activated T cells recruit exosomes secreted by dendritic cells via LFA-1. *Blood.* 2009; 113(9):1977–81. [PubMed: 19064723]
29. Chu K, Cheng CJ, Ye X, Lee YC, Zurita AJ, Chen DT, Yu-Lee LY, Zhang S, Yeh ET, Hu MC, Logothetis CJ, Lin SH. Cadherin-11 promotes the metastasis of prostate cancer cells to bone. *Mol Cancer Res.* 2008; 6(8):1259–67. [PubMed: 18708358]
30. Chen N, Ye XC, Chu K, Navone NM, Sage EH, Yu-Lee LY, Logothetis CJ, Lin SH. A secreted isoform of ErbB3 promotes osteonectin expression in bone and enhances the invasiveness of prostate cancer cells. *Cancer Res.* 2007; 67:6544–8. [PubMed: 17638862]
31. Gordon JA, Sodek J, Hunter GK, Goldberg HA. Bone sialoprotein stimulates focal adhesion-related signaling pathways: role in migration and survival of breast and prostate cancer cells. *J Cell Biochem.* 2009; 107(6):1118–28. [PubMed: 19492334]
32. Jacob K, Webber M, Benayahu D, Kleinman HK. Osteonectin promotes prostate cancer cell migration and invasion: a possible mechanism for metastasis to bone. *Cancer Res.* 1999; 59:4453–4457. [PubMed: 10485497]
33. Khodavirdi AC, Song Z, Yang S, Zhong C, Wang S, Wu H, Pritchard C, Nelson PS, Roy-Burman P. Increased expression of osteopontin contributes to the progression of prostate cancer. *Cancer Res.* 2006; 66:883–8. [PubMed: 16424021]
34. Villarroya-Beltri C, Baixauli F, Gutierrez-Vazquez C, Sanchez-Madrid F, Mittelbrunn M. Sorting it out: regulation of exosome loading. *Semin Cancer Biol.* 2014; 28:3–13. [PubMed: 24769058]

**Figure 1.**

Preparation of osteosomes from undifferentiated (D0) and differentiated (D24). (A) Experimental scheme for the isolation and characterization of exosomes from primary mouse osteoblasts, here termed “osteosomes”. (B) Morphology of D0 undifferentiated and D24 differentiated osteoblasts in culture. (C) Von Kossa stain for the mineralization of osteoblasts cultured in the absence (D0) or presence (D24) of differentiation medium. (D) Alizarin Red stain for mineralization of osteoblasts. Right panel, enlarged image of Alizarin Red staining of D24 differentiated osteoblasts. (E) Real-time RT-PCR for the expression of osteoblast differentiation markers, including alkaline phosphatase, osteocalcin, dentin matrix phosphoprotein-1, and sclerostin in D0 and D24 osteoblasts. Real-time RT-PCRs were performed on total RNAs prepared from calvarial osteoblasts cultured in the absence (D0) or

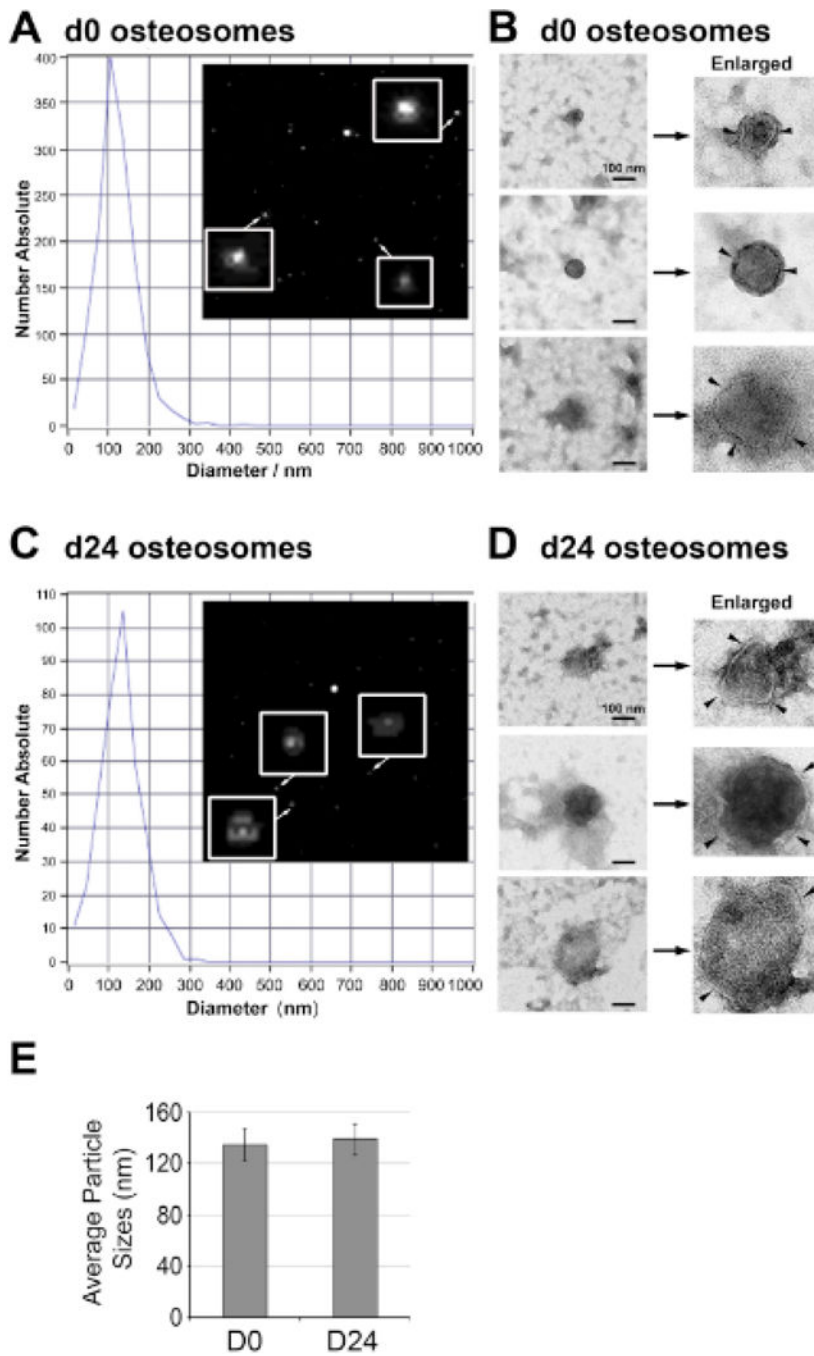
presence (D24) of osteoblast differentiation medium using gene-specific primers as indicated.

Author Manuscript

Author Manuscript

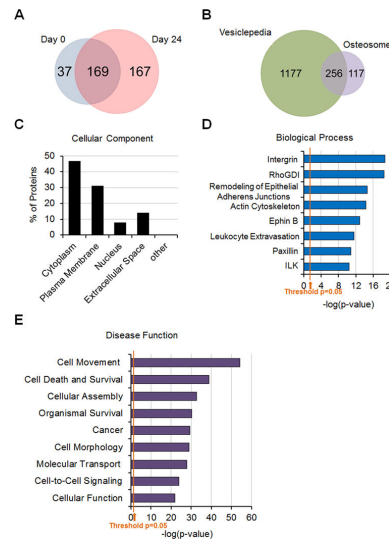
Author Manuscript

Author Manuscript

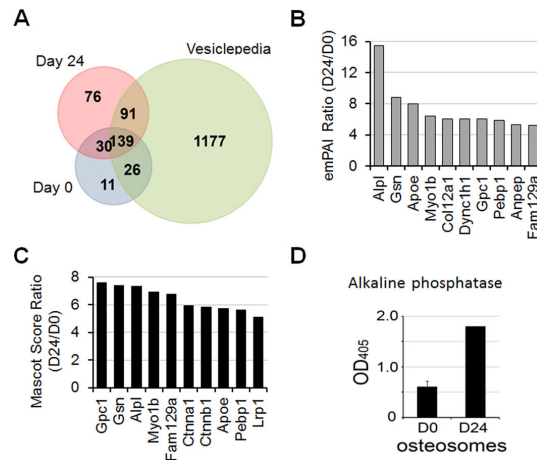
**Figure 2.**

Characterization of osteosomes. (A) Particle size and images of D0 osteosomes by dynamic light scattering analysis using a Zetasizer Nano ZS instrument. Osteosomes (see enlarged in insets) were found to be mainly ~50–150 nm size particles. (B) Transmission electron microscopy images of three representative D0 osteosomes were found to exhibit cup-shaped morphology (arrowheads) characteristic of exosomes. (C) Particle size and images of D24 osteosomes by dynamic light scattering analysis as in A. (D) Three representative transmission electron microscopy images of D24 osteosomes. Scale bar, 100 nm. (E)

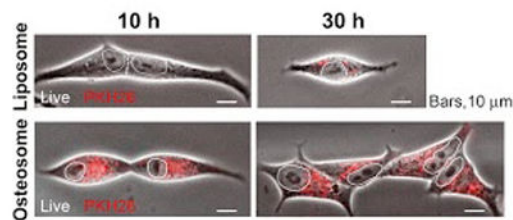
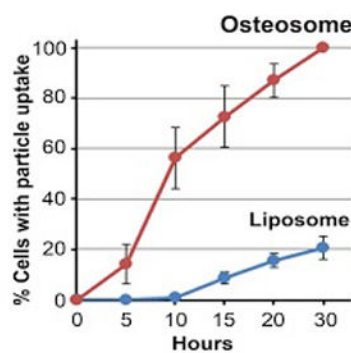
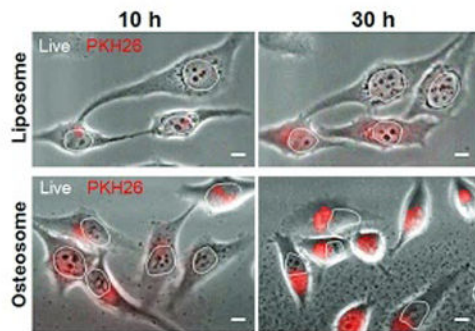
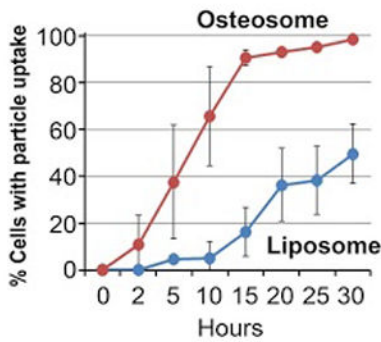
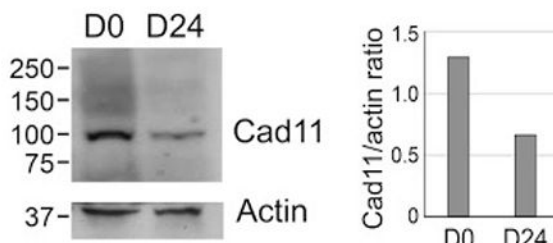
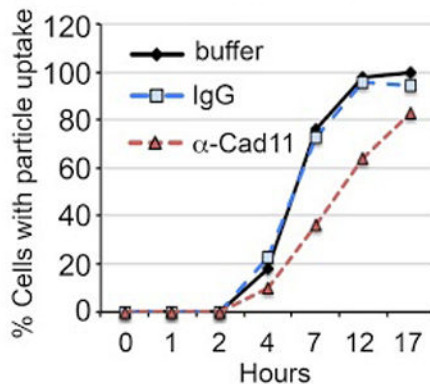
Average sizes of osteosomes from D0 and D24 osteoblasts. N=4. Data represent average \pm sem.

**Figure 3.**

Proteomics analysis of osteosomes. (A) Venn diagram of proteins in D0 vs D24 osteosoms. (B) Venn diagram of proteins in osteosomes and in Vesiclepedia. (C) Ingenuity Pathway Analysis of the intracellular origin of osteosome proteins. (D) The involvement of osteosome proteins in various biological processes. (E) The involvement of osteosome proteins in disease functions. These pathways are selected based on p values (expressed as $-\log(p\text{-value})$). The marked thresholds in D and E represent $p=0.05$.

**Figure 4.**

Comparison of proteomics profile of D0 and D24 osteosomes. (A) Venn diagram of proteins in D0, D24 osteosoms versus those in Vesiclepedia. (B) Proteins that showed a more or equal to 5-fold increase, based on emPAI values, in D24 osteosomes when compared to D0 osteosomes. (C) Proteins that showed a more or equal to 5-fold increase, based on protein score, in D24 osteosomes when compared to D0 osteosomes. (D) Enzymatic activity of alkaline phosphatase in D0 and D24 osteosomes.

A C4-2b**B PC3-mm2****C osteosomes****D PC3-mm2****Figure 5.**

Osteosome uptake into C4-2b and PC3-mm2 cells. Live-cell imaging of osteosome uptake in (A) C4-2b cells and (B) PC3-mm2 cells. Cells (1×10^4) were incubated with PKH26-labeled D24 osteosomes or PKH26-labeled control liposomes (3×10^5 particles). Live-cell imaging was recorded at 30 min intervals over 30 h on a Nikon Biostation. Number of cells imaged live: C4-2b with osteosome (n=157) or liposome (n=48); PC3-mm2 with osteosome (n=118) or liposome (n=100) in two independent experiments. Error bars, mean \pm s.d. Right panels, representative bright field images merged with PKH26 red fluorescence of cells treated with

PKH26-labeled liposomes or PKH26-labeled osteosomes. Nuclei are outlined; dash line separates two cells. Bars, 10 μ m. (C) Western blot of adhesion molecule cadherin-11 (Cad11) in D0 and D24 osteosomes. Right panel, quantification of Cad11 level. (D) Live-cell imaging of PC3-mm2 was performed as in B, except that PKH26-labeled osteosomes were preincubated with either anti-Cad11 mAb 1A5, isotype-matched irrelevant mAb (IgG), or PBS buffer, prior to their addition to cells. The final antibody concentration was 3 μ g/ml. Number of cells imaged live following osteosome pre-incubation with: PBS (n=55), IgG (n = 52), and Cad11 mAb (n=81).

Proteins common to D0 and D24 osteosomes

Table 1

prot_acc	GN	prot_desc	prot_mass (Da)	prot_score (Day 0)	prot_score (Day 24)	Num. of significant matches (day 0)	Num. of significant matches (day 24)	Number of unique peptide (day 0)	Number of unique peptide (day 24)	Sequence coverage (day 0)	Sequence coverage (day 24)
A2MG_MOUSE	A2m	Alpha-2-macroglobulin-P OS=Mus musculus GN=A2m PE=2 SV=2	164248	79	118	7	12	2	3	1.8	2.4
SYAC_MOUSE	Aars	Alanine-tRNA ligase, cytoplasmic OS=Mus musculus GN=Aars PE=1 SV=-1	106341	57	36	2	1	2	1	3.7	1
ACTB_MOUSE	Actb	Actin, cytoplasmic 1 OS=Mus musculus GN=Actb PE=1 SV=-1	41710	995	1160	95	88	18	19	62.9	62.9
ACTC_MOUSE	Actc1	Actin, alpha cardiac muscle 1 OS=Mus musculus GN=Actc1 PE=1 SV=-1	41992	710	670	63	48	15	13	55.4	48
ACTN1_MOUSE	Actn1	Alpha-actinin-1 OS=Mus musculus GN=Actn1 PE=1 SV=-1	103004	176	446	4	9	3	7	3.9	9.2
ARP3_MOUSE	Actr3	Actin-related protein 3 OS=Mus musculus GN=Actr3 PE=1 SV=3	47327	95	90	2	2	2	2	4.8	4.8
ALBU_MOUSE	Alb	Serum albumin OS=Mus musculus GN=Alb PE=-1 SV=3	68648	128	121	10	10	1	1	2.1	2.1
ALDOA_MOUSE	Aldoa	Fructose-bisphosphate aldolase A OS=Mus musculus GN=Aldoa PE=1 SV=2	39331	206	144	5	4	5	4	14.3	14
PPBT_MOUSE	Alpl	Alkaline phosphatase, tissue- nonspecific isozyme OS=Mus musculus GN=Alpl PE=1 SV=2	57478	120	879	3	81	2	15	4.8	35.7
AMPN_MOUSE	Anpep	Aminopeptidase N OS=Mus musculus GN=Anpep PE=1 SV=4	109582	159	753	5	30	4	16	6	25.6
ANXA1_MOUSE	Anxa1	Annexin A1 OS=Mus musculus GN=Anxa1 PE=1 SV=2	38710	508	822	15	38	8	13	29.5	41.9

prot_acc	GN	prot_desc	prot_mass (Da)	prot_score (Day 0)	prot_score (Day 24)	Num. of significant matches (day 0)	Num. of significant matches (day 24)	Number of unique peptide (day 0)	Number of unique peptide (day 24)	Sequence coverage (day 0)	Sequence coverage (day 24)
ANXA2_MOUSE	Anxa2	Annexin A2 OS=Mus musculus GN=Anxa2 PE=1 SV=2	38652	683	834	47	63	12	14	36	46.9
ANXA3_MOUSE	Anxa3	Annexin A3 OS=Mus musculus GN=Anxa3 PE=1 SV=4	36362	65	50	2	1	2	1	7.4	5
ANXA4_MOUSE	Anxa4	Annexin A4 OS=Mus musculus GN=Anxa4 PE=1 SV=4	35893	214	684	7	23	4	8	16.6	29.5
ANXA5_MOUSE	Anxa5	Annexin A5 OS=Mus musculus GN=Anxa5 PE=1 SV=-1	35730	581	1208	26	71	12	22	42	67.1
ANXA6_MOUSE	Anxa6	Annexin A6 OS=Mus musculus GN=Anxa6 PE=1 SV=3	75837	495	1026	18	47	11	22	23.2	42.1
AP2A1_MOUSE	Ap2a1	AP-2 complex subunit alpha-1 OS=Mus musculus GN=Ap2a1 PE=1 SV=1	107596	34	40	1	1	1	1	0.9	0.9
APOE_MOUSE	Apoe	Apolipoprotein E OS=Mus musculus GN=Apoe PE=1 SV=2	35844	108	619	4	23	3	12	10	35
ARF1_MOUSE	Arf1	ADP-ribosylation factor 1 OS=Mus musculus GN=Arf1 PE=1 SV=2	20684	265	203	11	9	6	4	43.6	32
ARF4_MOUSE	Arf4	ADP-ribosylation factor 4 OS=Mus musculus GN=Arf4 PE=1 SV=2	20384	104	106	3	5	3	2	23.3	11.7
ARF6_MOUSE	Arf6	ADP-ribosylation factor 6 OS=Mus musculus GN=Arf6 PE=1 SV=2	20069	50	82	2	4	1	2	5.7	12
GDIR1_MOUSE	Arhgdia	Rho GDP-dissociation inhibitor 1 OS=Mus musculus GN=Arhgdia PE=1 SV=3	23393	106	121	3	5	2	2	15.2	15.2
AT1A1_MOUSE	Atp1a1	Sodium/potassium ⁺ -transporting ATPase subunit alpha-1 OS=Mus musculus GN=Atp1a1 PE=1 SV=1	112910	616	972	20	35	13	17	18.5	23
AT2B1_MOUSE	Atp2b1	Plasma membrane calcium-transporting ATPase 1	134662	61	222	2	6	2	5	2.3	5.9

prot_acc	GN	prot_desc	prot_mass (Da)	prot_score (Day 0)	prot_score (Day 24)	Num. of significant matches (day 0)	Num. of significant matches (day 24)	Number of unique peptide (day 0)	Number of unique peptide (day 24)	Sequence coverage (day 0)	Sequence coverage (day 24)
B2MG_MOUSE	B2m	OS=Mus musculus GN=Atp2b1 PE=1 SV=1	13770	59	110	2	10	2	2	16	16
BASP1_MOUSE	Basp1	Beta-2-microglobulin OS=Mus musculus GN=B2m PE=1 SV=2	22074	364	321	11	7	8	6	51,3	38,1
BAS1_MOUSE	Bsg	Brain acid soluble protein 1 OS=Mus musculus GN=Basp1 PE=1 SV=3	42418	166	77	9	7	4	2	10,3	9,5
CO3_MOUSE	C3	Basigin OS=Mus musculus GN=Bsg PE=1 SV=2	186366	111	189	3	5	3	5	1,5	3,3
CALM_MOUSE	Calm1	Calmodulin OS=Mus musculus GN=Calm1 PE=1 SV=2	16327	293	272	16	21	5	5	38,3	38,3
CAP1_MOUSE	Cap1	Adenyl cyclase-associated protein 1 OS=Mus musculus GN=Cap1 PE=1 SV=4	51532	32	102	1	4	1	3	1,7	12,4
CSKP_MOUSE	Cask	Peripheral plasma membrane protein CASK OS=Mus musculus GN=Cask PE=1 SV=2	105042	94	86	3	2	3	2	3,7	1,7
TCPB_MOUSE	Cct2	T-complex protein 1 subunit beta OS=Mus musculus GN=Cct2 PE=1 SV=4	57441	89	79	2	2	2	2	6,9	5,6
CD44_MOUSE	Cd44	CD44 antigen OS=Mus musculus GN=Cd44 PE=1 SV=3	85365	78	62	3	3	1	1	1,5	1,5
CD47_MOUSE	Cd47	Leukocyte surface antigen CD47 OS=Mus musculus GN=Cd47 PE=1 SV=2	33076	42	77	1	1	1	1	4,6	4,6
CD81_MOUSE	Cd81	CD81 antigen OS=Mus musculus GN=Cd81 PE=1 SV=2	25797	62	94	4	6	1	1	8,5	8,5
CDCA2_MOUSE	Cdc42	Cell division control protein 42 homolog OS=Mus musculus GN=Cdc42 PE=1 SV=2	21245	172	211	7	9	4	4	25,7	25,7

prot_acc	GN	prot_desc	prot_mass (Da)	prot_score (Day 0)	prot_score (Day 24)	Num. of significant matches (day 0)	Num. of significant matches (day 24)	Number of unique peptide (day 0)	Number of unique peptide (day 24)	Sequence coverage (day 0)	Sequence coverage (day 24)
CAD11_MOUSE	Cdh11	Cadherin-11 OS=Mus musculus GN=Cdh11 PE=1 SV=1	88058	30	69	1	2	1	2	1.3	2.3
COFL1_MOUSE	Cfl1	Cofilin-1 OS=Mus musculus GN=Cfl1 PE=1 SV=3	18548	253	375	12	13	5	8	46.4	43.4
CLIC1_MOUSE	Clc1	Chloride intracellular channel protein 1 OS=Mus musculus GN=Clc1 PE=1 SV=3	26996	60	103	2	3	2	3	10.8	14.1
CLIC4_MOUSE	Clc4	Chloride intracellular channel protein 4 OS=Mus musculus GN=Clc4 PE=1 SV=3	28711	90	170	3	5	3	4	16.6	19.8
CLH1_MOUSE	Clc	Clathrin heavy chain 1 OS=Mus musculus GN=Clc PE=1 SV=3	191435	221	555	7	14	6	12	6.1	10.1
COCA1_MOUSE	Col12a1	Collagen alpha-1(XII) chain OS=Mus musculus GN=Col12a1 PE=2 SV=3	340004	45	115	1	4	1	4	0.3	1.3
COLA1_MOUSE	Colla1	Collagen alpha-1(I) chain OS=Mus musculus GN=Colla1 PE=1 SV=4	137948	1728	539	76	27	38	10	42	8.5
COLA2_MOUSE	Colla2	Collagen alpha-2(I) chain OS=Mus musculus GN=Colla2 PE=1 SV=2	129478	996	608	35	25	25	10	29.5	9.9
CTNNA1_MOUSE	Ctnna1	Catenin alpha-1 OS=Mus musculus GN=Ctnna1 PE=1 SV=1	100044	52	309	2	8	2	7	5	12.6
CTNBL1_MOUSE	Ctnnb1	Catenin beta-1 OS=Mus musculus GN=Ctnnb1 PE=1 SV=1	85416	55	321	2	10	2	7	3.3	12.4
DDAH1_MOUSE	Ddah1	NG,N(G)-dimethylarginine dimethylaminohydrolase 1 OS=Mus musculus GN=Ddah1 PE=1 SV=3	31361	52	49	2	1	2	1	7	3.5
DEST_MOUSE	Dstn	Destatin OS=Mus musculus GN=Dstn PE=1 SV=3	18509	61	79	2	2	2	2	10.9	14.5
DYHCH1_MOUSE	Dync1h1	Cytoplasmic dynein 1 heavy chain 1 OS=Mus musculus GN=Dync1h1 PE=1 SV=2	531710	44	200	1	6	1	6	0.3	1.8

prot_acc	GN	prot_desc	prot_mass (Da)	prot_score (Day 0)	prot_score (Day 24)	Num. of significant matches (day 0)	Num. of significant matches (day 24)	Number of unique peptide (day 0)	Number of unique peptide (day 24)	Sequence coverage (day 0)	Sequence coverage (day 24)
EDIL3_MOUSE	Edil3	EGF-like repeat and discoidin I-like domain-containing protein 3 OS=Mus musculus GN=Edil3 PE=1 SV=2	53677	780	678	75	50	16	13	37.9	34
EF1A1_MOUSE	Eef1a1	Elongation factor 1-alpha 1 OS=Mus musculus GN=Eef1a1 PE=1 SV=3	50082	369	438	24	32	7	9	19.3	22.5
EF2_MOUSE	Eef2	Elongation factor 2 OS=Mus musculus GN=Eef2 PE=1 SV=2	95253	220	326	6	9	6	9	10.5	13.5
EHDL_MOUSE	Ehd1	EH domain-containing protein 1 OS=Mus musculus GN=Ehd1 PE=1 SV=1	60365	105	147	2	5	2	3	7.1	8.4
EIF5A1_MOUSE	Eif5a	Eukaryotic translation initiation factor 5A-1 OS=Mus musculus GN=Eif5a PE=1 SV=2	16821	78	82	3	2	2	2	22.7	22.7
ENOA_MOUSE	Eno1	Alpha-enolase OS=Mus musculus GN=Eno1 PE=1 SV=3	47111	630	508	28	23	12	10	33.6	30.9
EZR1_MOUSE	Ezr	Ezrin OS=Mus musculus GN=Ezr PE=1 SV=3	69364	222	233	9	8	6	6	13.1	11.4
FABP5_MOUSE	Fabp5	Fatty acid-binding protein, epidermal OS=Mus musculus GN=Fabp5 PE=1 SV=3	15127	32	66	1	1	1	1	6.7	6.7
NIBAN_MOUSE	Fam129_a	Protein Niban OS=Mus musculus GN=Fam129a PE=1 SV=2	102585	60	405	2	14	2	9	2.8	12.7
FARP1_MOUSE	Farp1	FERM, RhoGEF and pleckstrin domain-containing protein 1 OS=Mus musculus GN=Farp1 PE=1 SV=1	118801	120	32	2	1	2	1	2.7	1
FLNA_MOUSE	Flna	Filamin-A OS=Mus musculus GN=Flna PE=1 SV=5	281046	234	163	6	5	5	4	2.3	1.5
FINC_MOUSE	Fn1	Fibronectin OS=Mus musculus GN=Fn1 PE=1 SV=4	272368	2549	2319	165	137	46	42	31.2	28.6

prot_acc	GN	prot_desc	prot_mass (Da)	prot_score (Day 0)	prot_score (Day 24)	Num. of significant matches (day 0)	Num. of significant matches (day 24)	Number of unique peptide (day 0)	Number of unique peptide (day 24)	Sequence coverage (day 0)	Sequence coverage (day 24)
FSCN1_MOUSE	Fscn1	Fascin OS=Mus musculus GN=Fscn1 PE=1 SV=4	54474	51	96	2	3	2	3	6.9	8.7
FRIL1_MOUSE	Ftl1	Ferritin light chain 1 OS=Mus musculus GN=Ftl1 PE=1 SV=2	20790	70	130	3	5	2	3	15.8	30.6
G3P_MOUSE	Gapdh	Glyceraldehyde-3-phosphate dehydrogenase OS=Mus musculus GN=Gapdh PE=1 SV=2	35787	439	369	24	21	8	8	34.5	42.9
SYG_MOUSE	Gars	Glycine-tRNA ligase OS=Mus musculus GN=Gars PE=1 SV=1	81826	35	94	1	3	1	3	1.4	5.3
GDIB_MOUSE	Gd12	Rab GDP dissociation inhibitor beta OS=Mus musculus GN=Gd12 PE=1 SV=1	50505	215	447	6	15	5	9	13.9	28.3
GNA12_MOUSE	Gna12	Guanine nucleotide-binding protein G(i) subunit alpha-2 OS=Mus musculus GN=Gna12 PE=1 SV=5	40463	321	556	14	32	6	9	24.8	33.5
GNAS1_MOUSE	Gnas	Guanine nucleotide-binding protein G(s) subunit alpha isoforms XLas OS=Mus musculus GN=Gnas PE=1 SV=1	121429	139	220	7	14	3	5	3.2	4.7
GBB1_MOUSE	Gnb1	Guanine nucleotide-binding protein G(I)/G(S)/G(T) subunit beta-1 OS=Mus musculus GN=Gnb1 PE=1 SV=3	37353	134	233	5	10	3	5	9.1	13.2
GBG12_MOUSE	Gng12	Guanine nucleotide-binding protein G(I)/G(S)/G(O) subunit gamma-12 OS=Mus musculus GN=Gng12 PE=1 SV=3	7992	142	100	3	2	3	2	47.2	25
GPC1_MOUSE	Gpc1	Glycican-1 OS=Mus musculus GN=Gpc1 PE=1 SV=1	61321	31	235	1	8	1	5	2.5	14
GELS_MOUSE	Gsn	Gelsolin OS=Mus musculus GN=Gsn PE=1 SV=3	85888	67	495	2	17	2	12	4.2	23.6

prot_acc	GN	prot_desc	prot_mass (Da)	prot_score (Day 0)	prot_score (Day 24)	Num. of significant matches (day 0)	Num. of significant matches (day 24)	Number of unique peptide (day 0)	Number of unique peptide (day 24)	Sequence coverage (day 0)	Sequence coverage (day 24)
GSTP1_MOUSE	Gsp1	Glutathione S-transferase P 1 OS=Mus musculus GN=Gsp1 PE=1 SV=2	23594	138	203	5	6	3	3	20.5	20.5
HA1B_MOUSE	H2-K1	H-2 class I histocompatibility antigen, K-B alpha chain OS=Mus musculus GN=H2-K1 PE=1 SV=1	41276	105	165	4	7	2	4	5.1	12.2
HBE_MOUSE	Hbb-y	Hemoglobin subunit epsilon-Y2 OS=Mus musculus GN=Hbb-y PE=1 SV=2	16126	52	38	5	5	1	1	6.8	6.8
HS90A_MOUSE	Hsp90aa1	Heat shock protein HSP 90-alpha OS=Mus musculus GN=Hsp90aa1 PE=1 SV=4	84735	230	355	7	8	6	8	10.6	13.2
HS90B_MOUSE	Hsp90a b1	Heat shock protein HSP 90-beta OS=Mus musculus GN=Hsp90ab1 PE=1 SV=3	83229	292	357	11	11	7	8	10.8	12
HSP7C_MOUSE	Hsp8	Heat shock cognate 71 kDa protein OS=Mus musculus GN=Hspas8 PE=1 SV=1	70827	593	784	23	29	15	17	29.3	35.3
PCBM_MOUSE	Hspg2	Basement membrane-specific heparan sulfate proteoglycan core protein OS=Mus musculus GN=Hsg2 PE=1 SV=-1	398039	892	242	29	5	20	5	7.6	1.4
IFIM2_MOUSE	Ifim2	Interferon-induced transmembrane protein 2 OS=Mus musculus GN=Ifim2 PE=1 SV=1	15733	34	40	2	5	1	1	5.6	5.6
IGSF8_MOUSE	Igsf8	Immunoglobulin superfamily member 8 OS=Mus musculus GN=Igsf8 PE=1 SV=2	64970	70	271	2	9	2	6	4.7	15.9
ILK_MOUSE	Ilk	Integrin-linked protein kinase OS=Mus musculus GN=Ilk PE=1 SV=2	51340	35	32	1	1	1	1	2.2	2.2
IQGAP1_MOUSE	Iqgap1	Ras GTPase-activating-like protein IQGAP1 OS=Mus musculus GN=Iqgap1 PE=1 SV=2	188624	226	407	5	9	5	9	4.4	9.2

prot_acc	GN	prot_desc	prot_mass (Da)	prot_score (Day 0)	prot_score (Day 24)	Num. of significant matches (day 0)	Num. of significant matches (day 24)	Number of unique peptide (day 0)	Number of unique peptide (day 24)	Sequence coverage (day 0)	Sequence coverage (day 24)
ITAV_MOUSE	Itgav	Integrin alpha-V OS=Mus musculus GN=Itgav PE=1 SV=2	115287	166	500	6	14	5	11	7.2	12
ITB1_MOUSE	Itgb1	Integrin beta-1 OS=Mus musculus GN=Itgb1 PE=1 SV=-1	88173	161	298	6	10	4	7	5.3	12.9
ITIH2_MOUSE	Itih2	Inter-alpha-trypsin inhibitor heavy chain H2 OS=Mus musculus GN=Itih2 PE=1 SV=-1	105861	272	471	10	17	6	8	6.7	9.3
ITIH3_MOUSE	Itih3	Inter-alpha-trypsin inhibitor heavy chain H3 OS=Mus musculus GN=Itih3 PE=1 SV=3	99296	42	72	1	3	1	2	1.1	2.7
IMB1_MOUSE	Kpnb1	Importin subunit beta-1 OS=Mus musculus GN=Kpnb1 PE=1 SV=2	97122	33	103	1	2	1	2	1.4	3.1
K1C10_MOUSE	Krt10	Keratin, type I cytoskeletal 10 OS=Mus musculus GN=Krt10 PE=1 SV=3	57735	333	79	29	3	6	2	10	3.7
K22E_MOUSE	Krt2	Keratin, type II cytoskeletal 2 epidermal OS=Mus musculus GN=Krt2 PE=1 SV=-1	70880	125	104	9	2	2	2	3.3	3.3
K2C5_MOUSE	Krt5	Keratin, type II cytoskeletal 5 OS=Mus musculus GN=Krt5 PE=1 SV=1	61729	208	60	9	2	3	1	5.7	2.1
K2C73_MOUSE	Krt73	Keratin, type II cytoskeletal 73 OS=Mus musculus GN=Krt73 PE=1 SV=-1	58875	168	128	8	5	2	2	4.3	4.3
K22O_MOUSE	Krt76	Keratin, type II cytoskeletal 2 oral OS=Mus musculus GN=Krt76 PE=1 SV=-1	62806	96	51	6	1	2	1	3.4	1.5
K2C79_MOUSE	Krt79	Keratin, type II cytoskeletal 79 OS=Mus musculus GN=Krt79 PE=1 SV=2	57517	88	77	2	2	1	2	2.3	4.3

prot_acc	GN	prot_desc	prot_mass (Da)	prot_score (Day 0)	prot_score (Day 24)	Num. of significant matches (day 0)	Num. of significant matches (day 24)	Number of unique peptide (day 0)	Number of unique peptide (day 24)	Sequence coverage (day 0)	Sequence coverage (day 24)
LAMP1_MOUSE	Lamp1	Lysosome-associated membrane glycoprotein 1 OS=Mus musculus GN=Lamp1 PE=1 SV=2	438337	117	218	5	9	3	4	7.6	11.3
LAMP2_MOUSE	Lamp2	Lysosome-associated membrane glycoprotein 2 OS=Mus musculus GN=Lamp2 PE=1 SV=2	45552	63	72	3	2	2	2	4.3	4.1
LDHA_MOUSE	Ldha	L-lactate dehydrogenase A chain OS=Mus musculus GN=Ldha PE=1 SV=3	36475	426	369	18	14	8	8	26.8	25.6
LEG1_MOUSE	Lgals1	Galecstin-1 OS=Mus musculus GN=Lgals1 PE=1 SV=3	14356	146	181	9	7	2	3	17.8	25.2
LRP1_MOUSE	Lrp1	Protein-density lipoprotein receptor-related protein 1 OS=Mus musculus GN=Lrp1 PE=1 SV=1	504411	39	198	1	4	1	4	0.2	0.9
LYZ2_MOUSE	Lyz2	Lysozyme C-2 OS=Mus musculus GN=Lyz2 PE=1 SV=2	16678	53	109	2	6	1	1	10.1	10.1
MARCS_MOUSE	Marcks	Myristoylated alanine-rich C-kinase substrate OS=Mus musculus GN=Marcks PE=1 SV=2	29644	173	201	8	10	4	4	16.8	16.8
MRP_MOUSE	Marcks1	MARCKS-related protein OS=Mus musculus GN=Marcks1 PE=1 SV=2	20153	77	59	2	1	2	1	14	6.5
MFGM_MOUSE	Mfge8	Lactadherin OS=Mus musculus GN=Mfge8 PE=1 SV=3	51208	895	1287	125	331	17	21	42.8	44.7
MIF_MOUSE	Mif	Macrophage migration inhibitory factor OS=Mus musculus GN=Mif PE=1 SV=2	12496	56	51	4	3	1	1	9.6	9.6
MOES_MOUSE	Msn	Moesin OS=Mus musculus GN=Msn PE=1 SV=3	67725	771	1229	38	47	19	28	35	45.2
MVP_MOUSE	Mvp	Major vault protein OS=Mus musculus GN=Mvp PE=1 SV=4	95365	62	156	2	4	2	4	2.7	6.2

prot_acc	GN	prot_desc	prot_mass (Da)	prot_score (Day 0)	prot_score (Day 24)	Num. of significant matches (day 0)	Num. of significant matches (day 24)	Number of unique peptide (day 0)	Number of unique peptide (day 24)	Sequence coverage (day 0)	Sequence coverage (day 24)
MYADM_MOUSE	Myadm	Myeloid-associated differentiation marker OS=Mus musculus GN=Myadm PE=1 SV=2	35261	69	77	5	5	1	1	5.3	5.3
MYH9_MOUSE	Myh9	Myosin-9 OS=Mus musculus GN=Myh9 PE=1 SV=4	226232	535	828	16	21	15	19	12.7	14.5
MYL6_MOUSE	Myl6	Myosin light polypeptide 6 OS=Mus musculus GN=Myl6 PE=1 SV=3	16919	57	138	2	4	2	4	15.9	29.1
MYO1B_MOUSE	Myo1b	Unconventional myosin-Ib OS=Myo1b PE=1 SV=3	128483	77	533	2	17	2	11	3.5	16.4
MYO1C_MOUSE	Myo1c	Unconventional myosin-Ic OS=Myo1c PE=1 SV=2	121868	338	595	12	20	9	15	13.8	17.7
NID2_MOUSE	Nid2	Nidogen-2 OS=Mus musculus GN=Nid2 PE=1 SV=2	153816	167	75	4	2	4	2	4.1	1.6
NDKA_MOUSE	Nmeli1	Nucleoside diphosphate kinase A OS=Mus musculus GN=Nmeli1 PE=1 SV=1	17197	31	68	2	5	1	2	11.2	21.1
PDC6L_MOUSE	Pded6ip	Programmed cell death 6-interacting protein OS=Mus musculus GN=Pded6ip PE=1 SV=3	95064	164	224	6	8	5	6	8.2	8.1
PEBP1_MOUSE	Pebp1	Phosphatidylethanolamine-binding protein 1 OS=Mus musculus GN=Pebp1 PE=1 SV=3	20817	33	185	1	5	1	4	13.9	32.6
PROF1_MOUSE	Pfn1	Profilin-1 OS=Mus musculus GN=Pfn1 PE=1 SV=2	14948	232	275	8	11	4	4	42.1	42.1
PI4KA_MOUSE	Pi4ka	Phosphatidylinositol 4-kinase alpha OS=Mus musculus GN=Pi4ka PE=1 SV=2	236889	43	60	1	1	1	1	0.6	0.6
KPYM_MOUSE	Pkm	Pyruvate kinase PKM OS=Mus musculus GN=Pkm PE=1 SV=4	57808	603	678	27	25	12	12	29.8	33
PLP2_MOUSE	Plp2	Protolipid protein 2 OS=Mus musculus GN=Plp2 PE=1 SV=1	16597	56	112	1	3	1	2	7.9	24.3

prot_acc	GN	prot_desc	prot_mass (Da)	prot_score (Day 0)	prot_score (Day 24)	Num. of significant matches (day 0)	Num. of significant matches (day 24)	Number of unique peptide (day 0)	Number of unique peptide (day 24)	Sequence coverage (day 0)	Sequence coverage (day 24)
PPIA_MOUSE	Ppia	Peptidyl-prolyl cis/trans isomerase A OS=Mus musculus GN=Ppia PE=1 SV=2	17960	212	239	12	16	6	6	31.7	34.8
2AAA_MOUSE	Ppp2r1a	Serine/threonine-protein phosphatase 2A 65 kDa regulatory subunit A alpha isoform OS=Mus musculus GN=Ppp2r1a PE=1 SV=3	65281	61	57	1	1	1	1	1.7	1.7
PRDX1_MOUSE	Prdx1	Peroxiredoxin-1 OS=Mus musculus GN=Prdx1 PE=1 SV=1	22162	108	288	4	12	3	8	16.1	40.2
PRDX2_MOUSE	Prdx2	Peroxiredoxin-2 OS=Mus musculus GN=Prdx2 PE=1 SV=3	21765	38	74	1	2	1	2	4	17.2
PRI0_MOUSE	Pnmp	Major prion protein OS=Mus musculus GN=Pnmp PE=1 SV=2	27960	33	81	1	2	1	2	3.5	7.1
PTK7_MOUSE	Ptk7	Inactive tyrosine-protein kinase / OS=Mus musculus GN=Ptk7 PE=1 SV=1	117457	284	181	12	5	8	4	11.7	5.6
RAB10_MOUSE	Rab10	Ras-related protein Rab-10 OS=Mus musculus GN=Rab10 PE=1 SV=1	22527	173	272	7	12	4	5	20	26
RAB14_MOUSE	Rab14	Ras-related protein Rab-14 OS=Mus musculus GN=Rab14 PE=1 SV=3	23382	83	191	5	8	2	4	8.4	19.1
RAP1A_MOUSE	Rap1a	Ras-related protein Rap-1A OS=Mus musculus GN=Rap1a PE=1 SV=1	20974	244	334	13	17	5	5	27.2	30.4
RAP2B_MOUSE	Rap2b	Ras-related protein Rap-2b OS=Mus musculus GN=Rap2b PE=1 SV=1	20491	43	83	1	2	1	2	6.6	20.8
RAD1_MOUSE	Rdx	Radixin OS=Mus musculus GN=Rdx PE=1 SV=3	68500	220	364	9	11	6	9	11.3	18.4
RHOA_MOUSE	Rhoa	Transforming protein RhoA OS=Mus musculus GN=Rhoa PE=1 SV=1	21768	118	201	2	11	2	4	13	31.6
RS27A_MOUSE	Rps27a	Ubiquitin-40S ribosomal protein S27a OS=Mus	17939	107	186	8	13	2	4	16	30.1

prot_acc	GN	prot_desc	prot_mass (Da)	prot_score (Day 0)	prot_score (Day 24)	Num. of significant matches (day 0)	Num. of significant matches (day 24)	Number of unique peptide (day 0)	Number of unique peptide (day 24)	Sequence coverage (day 0)	Sequence coverage (day 24)
RS8_MOUSE	Rps8	musculus GN=Rps27a PE=1 SV=2	24190	34	39	1	1	1	1	4.3	4.3
RRAS_MOUSE	Rras	40S ribosomal protein S8 OS=Mus musculus GN=Rps8 PE=1 SV=2	23749	90	147	2	4	2	4	10.6	21.1
RRAS2_MOUSE	Rras2	Ras-related protein R-Ras2 OS=Mus musculus GN=Rras2 PE=1 SV=1	23385	120	173	2	4	2	4	13.7	23.5
S10AA_MOUSE	S100a10	Protein S100-A10 OS=Mus musculus GN=S100a10 PE=1 SV=2	11179	74	97	4	6	2	2	35.1	35.1
S10AB_MOUSE	S100a11	Protein S100-A11 OS=Mus musculus GN=S100a11 PE=1 SV=1	11075	66	111	2	3	1	1	16.3	16.3
S10A4_MOUSE	S100a4	Protein S100-A4 OS=Mus musculus GN=S100a4 PE=1 SV=1	11714	41	135	1	3	1	3	8.9	17.8
S10A6_MOUSE	S100a6	Protein S100-A6 OS=Mus musculus GN=S100a6 PE=1 SV=3	10044	107	147	4	3	3	3	47.2	47.2
SH3L3_MOUSE	Sh3ngrl3	SH3 domain-binding glutamic acid-rich-like protein 3 OS=Mus musculus GN=Sh3ngrl3 PE=1 SV=1	10470	43	40	1	1	1	1	10.8	10.8
MOT1_MOUSE	Slc16a1	Monocarboxylate transporter 1 OS=Mus musculus GN=Slc16a1 PE=1 SV=1	53232	116	129	3	3	2	2	4.3	4.3
SATT_MOUSE	Slc1a4	Neutral amino acid transporter A OS=Mus musculus GN=Slc1a4 PE=1 SV=1	56026	66	39	2	1	2	1	3.6	2.1
4F2_MOUSE	Slc3a2	4F2 cell-surface antigen heavy chain OS=Mus musculus GN=Slc3a2 PE=1 SV=1	58300	454	325	13	9	9	8	20.7	16.9
LAT1_MOUSE	Slc7a5	Large neutral amino acids transporter small subunit 1	55836	233	213	7	5	4	4	16	16

prot_acc	GN	prot_desc	prot_mass (Da)	prot_score (Day 0)	prot_score (Day 24)	Num. of significant matches (day 0)	Num. of significant matches (day 24)	Number of unique peptide (day 0)	Number of unique peptide (day 24)	Sequence coverage (day 0)	Sequence coverage (day 24)
TAGL_MOUSE	Tagln	OS=Mus musculus GN=Slc7a5 PE=1 SV=2	22561	36	62	1	2	1	2	6.5	10
TFR1_MOUSE	Tfrc	Transferrin receptor protein 1 OS=Mus musculus GN=Tfrc PE=1 SV=1	85677	179	158	10	6	4	4	6	5.8
THY1_MOUSE	Thy1	Thy-1 membrane glycoprotein OS=Mus musculus GN=Thy1 PE=1 SV=1	18069	66	189	6	20	2	4	15.4	23.5
TLN1_MOUSE	Tln1	Talin-1 OS=Mus musculus GN=Tln1 PE=1 SV=2	269653	107	352	2	7	2	7	1	3.4
TYB4_MOUSE	Tmsb4x	Thymosin beta-4 OS=Mus musculus GN=Tmsb4x PE=1 SV=1	5676	32	33	1	1	1	1	14	14
TENA_MOUSE	Tnc	Tenascin OS=Mus musculus GN=Tnc PE=1 SV=1	231659	209	84	5	2	5	2	3.8	2.5
TPIS_MOUSE	Tpil	Triosephosphate isomerase OS=Mus musculus GN=Tpil PE=1 SV=4	32171	214	185	7	5	5	4	20.4	15.7
TPM4_MOUSE	Tpm4	Tropomyosin alpha-4 chain OS=Mus musculus GN=Tpm4 PE=1 SV=3	28450	71	117	2	3	2	3	14.9	18.1
TBA1A_MOUSE	Tubala	Tubulin alpha-1A chain OS=Mus musculus GN=Tubala PE=1 SV=1	50104	391	323	11	9	7	5	22.2	17.3
TBB5_MOUSE	Tubb5	Tubulin beta-5 chain OS=Mus musculus GN=Tubb5 PE=1 SV=1	49639	472	449	22	24	9	10	26.4	31.3
UBE2N_MOUSE	Ube2n	Ubiquitin-conjugating enzyme E2 N OS=Mus musculus GN=Ube2n PE=1 SV=1	17127	41	60	1	1	1	1	7.2	7.2
VAMP1_MOUSE	Vamp1	Vesicle-associated membrane protein 1 OS=Mus musculus GN=Vamp1 PE=1 SV=1	12382	32	43	1	1	1	1	5.9	5.9
VAT1_MOUSE	Vat1	Synaptic vesicle membrane protein VAT-1 homolog	43069	252	345	14	16	7	7	28.8	23.4

prot_acc	GN	prot_desc	prot_mass (Da)	prot_score (Day 0)	prot_score (Day 24)	Num. of significant matches (day 0)	Num. of significant matches (day 24)	Number of unique peptide (day 0)	Number of unique peptide (day 24)	Sequence coverage (day 0)	Sequence coverage (day 24)
VINC_MOUSE	Vcl	OS=Mus musculus GN=Vat1 PE=1 SV=3	116644	60	286	2	8	2	8	3.3	9.9
TERA_MOUSE	Vcp	Transitional endoplasmic reticulum ATPase OS=Mus musculus GN=Vcp PE=1 SV=4	89266	71	277	2	8	2	7	4	13
VIME_MOUSE	Vim	Vimentin OS=Mus musculus GN=Vim PE=1 SV=3	53655	358	349	11	11	8	8	19.1	16.1
WDR1_MOUSE	Wdr1	WD repeat-containing protein 1 OS=Mus musculus GN=Wdr1 PE=1 SV=3	66365	67	36	3	1	2	1	4	1.3
YKT6_MOUSE	Ykt6	Synaptobrevin homolog Ykt6 OS=Mus musculus GN=ykt6 PE=1 SV=1	22300	52	33	2	1	2	1	9.1	4.5
1433B_MOUSE	Ywhab	14-3-3 protein beta/alpha OS=Ywhab PE=1 SV=3	28069	241	299	6	9	5	6	18.3	24
1433E_MOUSE	Ywhae	14-3-3 protein epsilon OS=Ywhae PE=1 SV=1	29155	214	555	9	20	5	10	21.6	45.5
1433G_MOUSE	Ywhag	14-3-3 protein gamma OS=Ywhag PE=1 SV=2	28285	346	446	11	14	8	9	31.2	35.2
1433F_MOUSE	Ywhah	14-3-3 protein eta OS=Mus musculus GN=Ywhah PE=1 SV=2	28194	195	267	6	7	4	6	15.9	22
1433T_MOUSE	Ywhaq	14-3-3 protein theta OS=Mus musculus GN=Ywhaq PE=1 SV=1	27761	226	249	6	6	4	4	15.9	15.9
1433Z_MOUSE	Ywhaz	14-3-3 protein zeta/delta OS=Mus musculus GN=Ywhaz PE=1 SV=1	27754	338	415	12	14	7	7	40.4	35.9

Proteins unique to D0 osteosomes.

Table 2

prot_ac	GN	prot_desc	prot_mass (Da)	prot_score	Number of significant matches	Number of significant peptide sequences	Sequence coverage
ARF2_MOUSE	Arf2	ADP-ribosylation factor 2 OS=Mus musculus GN=Arf2 PE=1 SV=2	20733	219	7	5	43.6
HS71A_MOUSE	Hspala	Heat shock 70 kDa protein 1A OS=Mus musculus GN=Hspala PE=1 SV=2	70036	197	6	4	7.6
K2CL_MOUSE	Krt1	Keratin, type II cytoskeletal 1 OS=Mus musculus GN=Krt1 PE=1 SV=4	65565	168	11	2	3.6
GNAI3_MOUSE	Gna13	Guanine nucleotide-binding protein G(k) subunit alpha OS=Mus musculus GN=Gna13 PE=1 SV=3	40512	144	8	3	11.6
KIC17_MOUSE	Krt17	Keratin, type I cytoskeletal 17 OS=Mus musculus GN=Krt17 PE=1 SV=3	48132	113	10	3	6.2
RALA_MOUSE	Rala	Ras-related protein Ral-A OS=Mus musculus GN=Rala PE=1 SV=1	23538	109	3	3	25.2
STOM_MOUSE	Stom	Erythrocyte band 7 integral membrane protein OS=Mus musculus GN=Stom PE=1 SV=3	31355	95	3	3	15.1
GNA12_MOUSE	Gna12	Guanine nucleotide-binding protein subunit alpha-12 OS=Mus musculus GN=Gna12 PE=1 SV=3	44067	85	5	2	5
GTR1_MOUSE	Slc2a1	Solute carrier family 2, facilitated glucose transporter member 1 OS=Mus musculus GN=Slc2a1 PE=1 SV=4	53949	81	4	2	3.7
PGAM1_MOUSE	Pgam1	Phosphoglycerate mutase 1 OS=Mus musculus GN=Pgam1 PE=1 SV=3	28814	78	1	1	7.1
AKA12_MOUSE	Akap12	A-kinase anchor protein 12 OS=Mus musculus GN=Akap12 PE=1 SV=1	180586	76	2	2	1.1
NID1_MOUSE	Nid1	Nidogen-1 OS=Mus musculus GN=Nid1 PE=1 SV=2	136450	65	1	1	1.4
RAP2C_MOUSE	Rap2c	Ras-related protein Rap-2c OS=Mus musculus GN=Rap2c PE=1 SV=1	20731	64	2	2	14.8
LAMA4_MOUSE	Lama4	Laminin subunit alpha-4 OS=Mus musculus GN=Lama4 PE=1 SV=2	201692	63	2	2	1.8
TTYH3_MOUSE	Ttyh3	Protein tweety homolog 3 OS=Mus musculus GN=Ttyh3 PE=1 SV=1	57677	61	1	1	2.7
ANT3_MOUSE	Serpinc1	Antithrombin-III OS=Mus musculus GN=Serpinc1 PE=1 SV=1	51971	60	2	2	6.2
APOM_MOUSE	Apom	Apolipoprotein M OS=Mus musculus GN=Apom PE=1 SV=1	21259	59	1	1	4.2

prot_acc	GN	prot_desc	prot_mass (Da)	prot_score	Number of significant matches	Number of significant peptide sequences	Sequence coverage
RS2_MOUSE	Rps2	40S ribosomal protein S2 OS=Mus musculus GN=Rps2 PE=1 SV=3	31212	51	1	1	4.4
GSLG1_MOUSE	Glg1	Golgi apparatus protein 1 OS=Mus musculus GN=Glg1 PE=1 SV=1	133646	46	1	1	0.9
GAPR1_MOUSE	Glipr2	Golgi-associated plant pathogenesis-related protein 1 OS=Mus musculus GN=Glipr2 PE=1 SV=3	17080	43	1	1	8.4
RAB5C_MOUSE	Rab5c	Ras-related protein Rab-5C OS=Mus musculus GN=Rab5c PE=1 SV=2	23398	43	1	1	6.5
S38A5_MOUSE	Slc38a5	Sodium-coupled neutral amino acid transporter 5 OS=Mus musculus GN=Slc38a5 PE=1 SV=1	52582	42	1	1	1.7
AK1A1_MOUSE	Akrl1a1	Alcohol dehydrogenase [NADP(+)] OS=Mus musculus GN=Akrl1a1 PE=1 SV=3	36564	39	1	1	5.8
SF3A3_MOUSE	Sf3a3	Splicing factor 3A subunit 3 OS=Mus musculus GN=Sf3a3 PE=1 SV=2	58805	39	1	1	1.4
CTR1_MOUSE	Slc7a1	High affinity cationic amino acid transporter 1 OS=Mus musculus GN=Slc7a1 PE=1 SV=1	67048	35	1	1	3.1
NCAM1_MOUSE	Neam1	Neural cell adhesion molecule 1 OS=Mus musculus GN=Ncam1 PE=1 SV=3	119353	34	1	1	0.6
RL18_MOUSE	Rpl8	60S ribosomal protein L8 OS=Mus musculus GN=Rpl8 PE=1 SV=2	28007	34	1	1	4.3
VATL_MOUSE	Apb6v0c	V-type proton ATPase 16 kDa proteolipid subunit OS=Mus musculus GN=Apb6v0c PE=1 SV=1	15798	33	1	1	20
EHD2_MOUSE	Ehd2	EH domain-containing protein 2 OS=Mus musculus GN=Ehd2 PE=1 SV=1	61136	33	1	1	2.8
H4_MOUSE	Hist1h4a	Histone H4 OS=Mus musculus GN=Hist1h4a PE=1 SV=2	11360	33	1	1	9.7
PLAK_MOUSE	Jup	Junction plakophilin OS=Mus musculus GN=Jup PE=1 SV=3	81749	33	1	1	2.4
PCDAA_MOUSE	Pedhal0	Protocadherin alpha-10 OS=Mus musculus GN=Pedhal0 PE=2 SV=1	101994	33	1	1	0.8
ASNS_MOUSE	Asns	Asparagine synthetase [glutamine-hydrolyzing] OS=Mus musculus GN=Asns PE=1 SV=3	64241	31	1	1	1.6
TCPZ_MOUSE	Cett6a	T-complex protein 1 subunit zeta OS=Mus musculus GN=Cett6a PE=1 SV=3	57968	31	1	1	3.2
RASH_MOUSE	Hras	GTPase HRas OS=Mus musculus GN=Hras PE=1 SV=2	21285	31	1	1	5.8
PARVA_MOUSE	Parva	Alpha-parvin OS=Mus musculus GN=Parva PE=1 SV=1	42304	31	1	1	3.8

prot_acc	GN	prot_desc	prot_mass (Da)	prot_score	Number of significant matches	Number of significant unique peptide sequences	Sequence coverage
PGK1_MOUSE	Pgk1	Phosphoglycerate kinase 1 OS=Mus musculus GN=Pgk1 PE=1 SV=4	44522	31	1	1	4.3

Proteins unique to D24 osteosomes

Table 3

prot_ac	GN	prot_desc	prot_mass (Da)	prot_seo_re	Number of significant matches	Number of significant peptide sequences	Sequence coverage
C06A1_MOUSE	Col6a1	Collagen alpha-1(VI) chain OS=Mus musculus GN=Col6a1 PE=1 SV=1	108422	1441	117	21	26
C06A2_MOUSE	Col6a2	Collagen alpha-2(VI) chain OS=Mus musculus GN=Col6a2 PE=1 SV=3	110266	871	50	19	23
FPRP_MOUSE	Pigfrn	Prostaglandin F2 receptor negative regulator OS=Mus musculus GN=Pigfrn PE=1 SV=2	98660	630	20	13	18.7
E41L2_MOUSE	Epb41l2	Band 4.1-like protein 2 OS=Mus musculus GN=Epb41l2 PE=1 SV=2	109873	603	19	14	16.8
PHEX_MOUSE	Phex	Metalloendopeptidase homolog PEX OS=Mus musculus GN=Phex PE=1 SV=1	86364	469	14	10	17.1
MYO1D_MOUSE	Myo1d	Unconventional myosin-Id OS=Mus musculus GN=Myo1d PE=1 SV=1	116007	393	12	11	12.8
PPIC_MOUSE	Ppic	Peptidyl-prolyl cis-trans isomerase C OS=Mus musculus GN=PPic PE=1 SV=1	22780	389	27	7	48.6
ACTN4_MOUSE	Actn4	Alpha-actinin-4 OS=Mus musculus GN=Actn4 PE=1 SV=1	104911	388	9	7	10.1
PLCD1_MOUSE	Plcd1	1-phosphatidylinositol 4,5-bisphosphate phosphodiesterase delta-1 OS=Mus musculus GN=Plcd1 PE=1 SV=2	85819	383	12	8	17.9
LUM_MOUSE	Lum	Lumican OS=Mus musculus GN=Lum PE=1 SV=2	38241	369	13	7	23.4
PHOPI_MOUSE	Phophoi	Phosphothanolamine/phosphocholine phosphatase OS=Mus musculus GN=Phosphi1 PE=1 SV=1	29892	311	12	7	31.5
IGSF8_MOUSE	Igsf8	Immunoglobulin superfamily member 8 OS=Mus musculus GN=Igsf8 PE=1 SV=2	64970	271	9	6	15.9
EMILIN1_MOUSE	Emilin1	EMILIN-1 OS=Mus musculus GN=Emilin1 PE=1 SV=1	107518	266	5	5	7.3
GBB2_MOUSE	Gnb2	Guanine nucleotide-binding protein G(I)/G(S)/G(T) subunit beta-2 OS=Mus musculus GN=Gnb2 PE=1 SV=3	37307	253	10	5	13.2
NEP_MOUSE	Mne	Neprilysin OS=Mus musculus GN=Mne PE=1 SV=3	85648	236	8	6	11.1
IDHC_MOUSE	Idh1	Isocitrate dehydrogenase [NADP] cytoplasmic OS=Mus musculus GN=Idh1 PE=1 SV=2	46644	226	5	5	17.1
RAB35_MOUSE	Rab35	Ras-related protein Rab-35 OS=Mus musculus GN=Rab35 PE=1 SV=1	23011	216	10	4	20.9
CATB_MOUSE	Ctsb	Cathepsin B OS=Mus musculus GN=Ctsb PE=1 SV=2	37256	205	5	4	15.9

prot_acc	GN	prot_desc	prot_mass (Da)	prot_secre	Number of significant matches	Number of significant peptide sequences	Sequence coverage
KADI_MOUSE	Akl	Adenylate kinase isoenzyme 1 OS=Mus musculus GN=Akl PE=1 SV=1	21526	203	5	4	20.6
CATD_MOUSE	Ctsd	Cathepsin D OS=Mus musculus GN=Ctsd PE=1 SV=1	44925	194	5	4	12.4
PEDF_MOUSE	Serpinfl	Pigment epithelium-derived factor OS=Mus musculus GN=Serpinf1 PE=1 SV=2	46205	194	8	5	21.3
ASM3B_MOUSE	Smpd13b	Acid sphingomyelinase-like phosphodiesterase 3b OS=Mus musculus GN=Smpd13b PE=1 SV=1	51567	180	4	4	14.7
CD109_MOUSE	Cd109	CD109 antigen OS=Mus musculus GN=Cd109 PE=1 SV=1	161557	174	5	4	3.6
AQP1_MOUSE	Aqp1	Aquaporin-1 OS=Mus musculus GN=Aqp1 PE=1 SV=3	28775	172	7	4	24.5
GNA11_MOUSE	Gna11	Guanine nucleotide-binding protein 11 OS=Mus musculus GN=Gna11 PE=1 SV=1	41997	169	5	5	17.5
TM119_MOUSE	Tmem119	Transmembrane protein 119 OS=Mus musculus GN=Tmem119 PE=1 SV=1	29383	161	20	4	15.7
AEBP1_MOUSE	Aebp1	Adipocyte enhancer-binding protein 1 OS=Mus musculus GN=Aebp1 PE=1 SV=1	128284	158	4	3	3.1
SDCB1_MOUSE	Sdcbp	Syntenin-1 OS=Mus musculus GN=Sdcbp PE=1 SV=1	32359	158	4	3	21.1
EHD3_MOUSE	Ehd3	EH domain-containing protein 3 OS=Mus musculus GN=Ehd3 PE=1 SV=2	60783	150	6	4	9
GSTM1_MOUSE	Gstml1	Glutathione S-transferase Mu 1 OS=Mus musculus GN=Gstml1 PE=1 SV=2	25953	142	4	3	17.4
FLNC_MOUSE	Flnc	Filamin-C OS=Mus musculus GN=Flnc PE=1 SV=3	290937	134	4	3	1.1
MMP14_MOUSE	Mmp14	Matrix metalloproteinase-14 OS=Mus musculus GN=Mmp14 PE=2 SV=3	65877	132	4	4	7.6
CTND1_MOUSE	Ctnnd1	Catenin delta-1 OS=Mus musculus GN=Ctnnd1 PE=1 SV=2	104860	126	3	3	5.1
AT2B4_MOUSE	Atp2b4	Plasma membrane calcium-transferring ATPase 4 OS=Mus musculus GN=Atp2b4 PE=1 SV=1	132984	125	4	3	3.7
NRP2_MOUSE	Nrp2	Neuropilin-2 OS=Mus musculus GN=Nrp2 PE=1 SV=2	104565	123	3	3	3.8
DLG1_MOUSE	Dlg1	Disk large homolog 1 OS=Mus musculus GN=Dlg1 PE=1 SV=1	100058	122	4	3	3.9
PANX3_MOUSE	Panx3	Pannexin-3 OS=Mus musculus GN=Panx3 PE=1 SV=1	44899	122	6	3	12.2
GDIA_MOUSE	Gdi1	Rab GDP dissociation inhibitor alpha OS=Mus musculus GN=Gdi1 PE=1 SV=3	50489	116	3	3	10.5
SAP_MOUSE	Psap	Prosaposin OS=Mus musculus GN=Psap PE=1 SV=2	61381	116	6	3	7.2

prot_acc	GN	prot_desc	prot_mass (Da)	prot_secre	Number of significant matches	Number of significant peptide sequences	Sequence coverage
DPYL2_MOUSE	Dpysl2	Dihydropyrimidinase-related protein 2 OS=Mus musculus GN=Dpysl2 PE=1 SV=2	62239	115	3	3	9.8
NSMA2_MOUSE	Smpd3	Sphingomyelin phosphodiesterase 3 OS=Mus musculus GN=Smpd3 PE=1 SV=1	71152	110	3	3	7.5
ANO6_MOUSE	Ano6	Anoctamin-6 OS=Mus musculus GN=Ano6 PE=1 SV=1	106186	108	3	3	3.4
MYOF_MOUSE	Myof	Myoferlin OS=Mus musculus GN=Myof PE=1 SV=2	233177	108	2	2	1
PLXB2_MOUSE	Pknb2	Plexin-B2 OS=Mus musculus GN=Pknb2 PE=1 SV=1	206099	108	2	2	1
C03A1_MOUSE	Col3a1	Collagen alpha-1 (III) chain OS=Mus musculus GN=Col3a1 PE=1 SV=4	138858	106	3	3	1.9
FERM2_MOUSE	Femt2	Fernitin family homolog 2 OS=Mus musculus GN=Ferm2 PE=1 SV=1	77750	106	3	3	5.6
TKT_MOUSE	Tkt	Transketolase OS=Mus musculus GN=Tkt PE=1 SV=1	67588	106	3	3	8.2
S13A5_MOUSE	Slc13a5	Solute carrier family 13 member 5 OS=Mus musculus GN=Slc13a5 PE=2 SV=1	63780	103	4	3	5.6
MMP2_MOUSE	Mmp2	72 kDa type IV collagenase OS=Mus musculus GN=Mmp2 PE=1 SV=1	74055	102	3	3	8.6
FMOD_MOUSE	Fmod	Fibromodulin OS=Mus musculus GN=Fmod PE=2 SV=1	43027	101	2	2	11.2
CAPG_MOUSE	Capg	Macrophage-capping protein OS=Mus musculus GN=Capg PE=1 SV=2	39216	97	2	2	8
UBA1_MOUSE	Uba1	Ubiquitin-like modifier-activating enzyme 1 OS=Mus musculus GN=Uba1 PE=1 SV=1	117734	97	2	2	1.9
DDAH2_MOUSE	Ddah2	(N(G)NG)-dimethylarginine dimethylaminohydrolase 2 OS=Mus musculus GN=Ddah2 PE=1 SV=1	29627	96	2	2	12.3
RB11A_MOUSE	Rab11a	Ras-related protein Rab-11A OS=Mus musculus GN=Rab11a PE=1 SV=3	24378	96	3	3	14.8
CA2D1_MOUSE	Cacna2d1	Voltage-dependent calcium channel subunit alpha-2/delta-1 OS=Mus musculus GN=Cacna2d1 PE=1 SV=1	124551	93	2	2	3.5
NUCB1_MOUSE	Nucb1	Nucleobindin-1 OS=Mus musculus GN=Nucb1 PE=1 SV=2	53376	93	2	2	4.4
ARF5_MOUSE	Arf5	ADP-ribosylation factor 5 OS=Mus musculus GN=Arf5 PE=1 SV=2	20517	90	5	2	11.7
PLTP_MOUSE	Ptp	Phospholipid transfer protein OS=Mus musculus GN=Ptp PE=1 SV=1	54419	89	2	2	6.3
TSP2_MOUSE	Thbs2	Thrombospondin-2 OS=Mus musculus GN=Thbs2 PE=1 SV=2	129798	89	2	2	3.2

prot_acc	GN	prot_desc	prot_mass (Da)	prot_secre	Number of significant matches	Number of significant peptide sequences	Sequence coverage
NDKB_MOUSE	Nme2	Nucleoside diphosphate kinase B OS=Mus musculus GN=Nme2 PE=1 SV=1	17352	84	6	2	23.7
PCBP1_MOUSE	Pcbp1	Poly(rC)-binding protein 1 OS=Mus musculus GN=Pcbp1 PE=1 SV=1	37474	83	2	2	5.3
NAC3_MOUSE	Slc8a3	Sodium/calcium exchanger 3 OS=Mus musculus GN=Slc8a3 PE=1 SV=1	102917	79	2	2	1.9
5NTD_MOUSE	Nt5e	5~-nucleotidase OS=Mus musculus GN=Nt5e PE=1 SV=2	63824	78	2	2	4.2
S12A2_MOUSE	Slc12a2	Solute carrier family 12 member 2 OS=Mus musculus GN=Slc12a2 PE=1 SV=2	130950	78	3	3	4.8
ANXA7_MOUSE	Anxa7	Annexin A7 OS=Mus musculus GN=Anxa7 PE=1 SV=2	49893	77	2	2	5.6
OX2G_MOUSE	Cd200	OX-2 membrane glycoprotein OS=Mus musculus GN=Cd200 PE=1 SV=1	31236	77	6	2	8.6
ENPP1_MOUSE	Enpp1	Ectonucleotide pyrophosphatase/phosphodiesterase family member 1 OS=Mus musculus GN=Enpp1 PE=1 SV=4	103109	76	2	2	4.1
FKB1A_MOUSE	Fkbp1a	Peptidyl-prolyl cis-trans isomerase FKBP1A OS=Mus musculus GN=Fkbp1a PE=1 SV=2	11915	76	1	1	13
CHP1_MOUSE	Chp1	Calneurin B homologous protein 1 OS=Mus musculus GN=Chp1 PE=1 SV=2	22418	75	2	2	11.8
CTL2_MOUSE	Slc44a2	Choline transporter-like protein 2 OS=Mus musculus GN=Slc44a2 PE=1 SV=2	80057	71	2	2	3.4
CHM4B_MOUSE	Chmp4b	Changed multivesicular body protein 4b OS=Mus musculus GN=Chmp4b PE=1 SV=2	24921	70	2	2	11.2
FA5_MOUSE	F5	Coagulation factor V OS=Mus musculus GN=F5 PE=1 SV=1	247076	70	2	2	1
KIC15_MOUSE	Krt15	Keratin, type I cytoskeletal 15 OS=Mus musculus GN=Krt15 PE=1 SV=2	49107	70	3	2	3.5
PLST_MOUSE	Pls3	Plastin-3 OS=Mus musculus GN=Pls3 PE=1 SV=3	70697	70	2	2	3.7
MRC2_MOUSE	Mrc2	C-type mannose receptor 2 OS=Mus musculus GN=Mrc2 PE=1 SV=3	166968	69	2	2	1.4
PRDX5_MOUSE	Prdx5	Peroxiredoxin-5, mitochondrial OS=Mus musculus GN=Prdx5 PE=1 SV=2	21884	69	2	1	8.1
SYTC_MOUSE	Tars	Threonyne-tRNA ligase, cytoplasmic OS=Mus musculus GN=Tars PE=1 SV=2	83303	69	2	2	2.2
KCY_MOUSE	Cnpk1	UMP-CMP kinase OS=Mus musculus GN=Cnpk1 PE=1 SV=1	22151	68	2	2	11.2
PSA5_MOUSE	Psma5	Proteasome subunit alpha type-5 OS=Mus musculus GN=Psma5 PE=1 SV=1	26394	68	1	1	5

prot_ac	GN	prot_desc	prot_mass (Da)	prot_secre	Number of significant matches	Number of significant peptide sequences	Sequence coverage
PKHO2_MOUSE	Plekho2	Pleckstrin homology domain-containing family O member 2 OS=Mus musculus GN=Plekho2 PE=1 SV=1	53839	67	1	1	2.4
CERU_MOUSE	Cp	Ceroplasmin OS=Mus musculus GN=Cp PE=1 SV=2	121074	62	2	2	3.1
DCTN1_MOUSE	Dcnl1	Dynactin subunit 1 OS=Mus musculus GN=Dcnl1 PE=1 SV=3	141588	62	1	1	0.9
DC112_MOUSE	Dync1i2	Cytoplasmic dynein 1 intermediate chain 2 OS=Mus musculus GN=Dync1i2 PE=1 SV=1	68332	62	1	1	1.6
HTRAL_MOUSE	Htral	Serine protease HTRA1 OS=Mus musculus GN=Htral PE=1 SV=2	511182	62	4	2	8.5
SERC5_MOUSE	Seric5	Serine incorporator 5 OS=Mus musculus GN=Seric5 PE=2 SV=1	51795	61	1	1	2
PRS8_MOUSE	Psmc5	26S protease regulatory subunit 8 OS=Mus musculus GN=Psmc5 PE=1 SV=1	45597	60	1	1	3.2
IFM5_MOUSE	Ifim5	Interferon-induced transmembrane protein 5 OS=Mus musculus GN=Ifim5 PE=1 SV=1	14657	59	2	1	6.7
TCPQ_MOUSE	Cct8	T-complex protein 1 subunit theta OS=Mus musculus GN=Cct8 PE=1 SV=3	59518	56	1	1	1.8
STEA3_MOUSE	Steap3	Metalloreductase STEAP3 OS=Mus musculus GN=Steap3 PE=1 SV=1	54714	56	3	1	2.7
APOB_MOUSE	Apob	Apolipoprotein B-100 OS=Mus musculus GN=Apob PE=1 SV=1	509113	55	1	1	0.3
CAD13_MOUSE	Cdh13	Cadherin-13 OS=Mus musculus GN=Cdh13 PE=1 SV=2	78137	54	1	1	1.7
MDHC_MOUSE	Mdh1	Malate dehydrogenase, cytoplasmic OS=Mus musculus GN=Mdh1 PE=1 SV=3	36488	53	1	1	3.9
CR1L_MOUSE	Cr1l	Complement component receptor 1-like protein OS=Mus musculus GN=Cr1l PE=1 SV=1	53728	52	1	1	2.3
TSN4_MOUSE	Tspan4	Tetraspanin-4 OS=Mus musculus GN=Tspan4 PE=1 SV=1	26036	52	2	1	10.5
ARPC2_MOUSE	Arpc2	Actin-related protein 2/3 complex subunit 2 OS=Mus musculus GN=Arpc2 PE=1 SV=3	34336	50	1	1	3.3
MUG1_MOUSE	Mug1	Murinoglobulin-1 OS=Mus musculus GN=Mug1 PE=1 SV=3	165193	50	2	1	0.5
DDAH1_MOUSE	Ddah1	N(G,N(G)-dimethylarginine dimethylaminohydrolase 1 OS=Mus musculus GN=Ddah1 PE=1 SV=3	31361	49	1	1	3.5
H2B1B_MOUSE	Hist1h2bb	Histone H2B type 1-B OS=Mus musculus GN=Hist1h2bb PE=1 SV=3	13944	49	1	1	11.9
NDRG1_MOUSE	Ndrg1	Protein NDRG1 OS=Mus musculus GN=Nrdg1 PE=1 SV=1	42981	49	1	1	3.6
CPNE1_MOUSE	Cpne1	Copine-1 OS=Mus musculus GN=Cpne1 PE=1 SV=1	58849	48	1	1	1.7

prot_acc	GN	prot_desc	prot_mass (Da)	prot_secre	Number of significant matches	Number of significant peptide sequences	Sequence coverage
PACN2_MOUSE	Pacsin2	Protein kinase C and casein kinase substrate in neurons protein 2 OS=Mus musculus GN=Pacsin2 PE=1 SV=1	55798	48	1	1	1.9
PSA2_MOUSE	Psma2	Proteasome subunit alpha type-2 OS=Mus musculus GN=Psma2 PE=1 SV=3	25910	46	1	1	9
RAB21_MOUSE	Rab21	Ras-related protein Rab-21 OS=Mus musculus GN=Rab21 PE=1 SV=4	24091	46	1	1	4.5
CLCA_MOUSE	Cltia	Clathrin light chain A OS=Mus musculus GN=Cltia PE=1 SV=2	25588	45	1	1	3.8
PCOCL_MOUSE	Pcolce	Procollagen C-endopeptidase enhancer 1 OS=Mus musculus GN=Pcolce PE=1 SV=2	50136	45	1	1	2.1
S29A1_MOUSE	Slc29a1	Equilibrative nucleoside transporter 1 OS=Mus musculus GN=Slc29a1 PE=1 SV=3	50159	45	2	1	2.6
CYTC_MOUSE	Cst3	Cystatin-C OS=Mus musculus GN=Cst3 PE=1 SV=2	15521	44	2	1	7.9
SYDC_MOUSE	Dars	Aspartate-tRNA ligase, cytoplasmic OS=Mus musculus GN=Dars PE=1 SV=2	57111	44	1	1	2
MAOX_MOUSE	Me1	NADP-dependent malic enzyme OS=Mus musculus GN=Me1 PE=1 SV=2	63913	44	1	1	3.1
RASA3_MOUSE	Rasa3	Ras GTPase-activating protein 3 OS=Mus musculus GN=Rasa3 PE=1 SV=2	95926	44	1	1	0.8
CD9_MOUSE	Cd9	CD9 antigen OS=Mus musculus GN=Cd9 PE=1 SV=2	25241	43	6	1	3.1
GBG5_MOUSE	Gng5	Guanine nucleotide-binding protein G(I)/G(S)/G(O) subunit gamma-5 OS=Mus musculus GN=Gng5 PE=1 SV=2	7314	43	1	1	13.2
PSD12_MOUSE	Psnd12	26S proteasome non-ATPase regulatory subunit 12 OS=Mus musculus GN=Psnd12 PE=1 SV=4	52861	43	1	1	2.2
PRS7_MOUSE	Psnc2	26S protease regulatory subunit 7 OS=Mus musculus GN=Psnc2 PE=1 SV=5	48617	42	1	1	3
RL15_MOUSE	Rpl15	60S ribosomal protein L15 OS=Mus musculus GN=Rpl15 PE=2 SV=4	24131	42	2	1	5.9
TENN_MOUSE	Tnn	Tenascin-N OS=Mus musculus GN=Tnn PE=1 SV=2	172983	42	1	1	0.6
PP2AA_MOUSE	Ppp2ca	Serine/threonine-protein phosphatase 2A catalytic subunit alpha isoform OS=Mus musculus GN=Ppp2ca PE=1 SV=1	35585	41	1	1	2.6
PSB6_MOUSE	Psmb6	Proteasome subunit beta type-6 OS=Mus musculus GN=Psmb6 PE=1 SV=3	25362	41	1	1	4.2
ROR1_MOUSE	Ror1	Inactive tyrosine-protein kinase transmembrane receptor ROR1 OS=Mus musculus GN=Ror1 PE=2 SV=2	104021	41	1	1	1.1

prot_acc	GN	prot_desc	prot_mass (Da)	prot_secre	Number of significant matches	Number of significant peptide sequences	Sequence coverage
NHRF1_MOUSE	Sle9a3rl	Na(+) / H(+) exchange regulatory cofactor NHE-RF1 OS=Mus musculus GN=Sle9a3rl PE=1 SV=3	38577	41	1	1	2.8
ANX11_MOUSE	Anxa11	Annexin A11 OS=Mus musculus GN=Anxa11 PE=1 SV=2	54045	40	1	1	2.4
CAPZB_MOUSE	Capzb	F-actin-capping protein subunit beta OS=Mus musculus GN=C Capzb PE=1 SV=3	31326	40	1	1	2.9
CHM1A_MOUSE	Chmp1a	Charged multivesicular body protein 1a OS=Mus musculus GN=Chmp1a PE=1 SV=1	21594	40	1	1	4.1
LIN7A_MOUSE	Lin7a	Protein lin-7 homolog A OS=Mus musculus GN=Lin7a PE=1 SV=2	25977	40	1	1	4.3
VNN1_MOUSE	Vnn1	Pantetheinase OS=Mus musculus GN=Ynn1 PE=1 SV=3	57054	40	2	1	2.5
CAN2_MOUSE	Capn2	Calpain-2 catalytic subunit OS=Mus musculus GN=Capn2 PE=1 SV=4	79822	39	1	1	1.1
EFR3A_MOUSE	Efr3a	Protein EFR3 homolog A OS=Mus musculus GN=Efr3a PE=1 SV=1	92554	39	1	1	1.3
FAS_MOUSE	Fasn	Fatty acid synthase OS=Mus musculus GN=Fasn PE=1 SV=2	272257	39	1	1	0.4
S39AA_MOUSE	Sle39a10	Zinc transporter ZIP10 OS=Mus musculus GN=Sle39a10 PE=1 SV=1	94335	39	1	1	1.2
VPS35_MOUSE	Vps35	Vacuolar protein sorting-associated protein 35 OS=Mus musculus GN=Vps35 PE=1 SV=1	91655	39	2	1	1.4
APOA1_MOUSE	Apoa1	Apolipoprotein A-I OS=Mus musculus GN=Apoa1 PE=1 SV=2	30597	38	2	1	3.8
F234A_MOUSE	Fam234a	Protein FAM234A OS=Mus musculus GN=Fam234a PE=1 SV=1	60538	38	1	1	1.8
SEPR_MOUSE	Fap	Prolyl endopeptidase FAP OS=Mus musculus GN=Fap PE=1 SV=1	87889	38	1	1	1.3
PTPRA_MOUSE	Ptpa	Receptor-type tyrosine-protein phosphatase alpha OS=Mus musculus GN=Ptpa PE=1 SV=3	93638	38	1	1	2.2
TCTP_MOUSE	Tpt1	Translationally-controlled tumor protein OS=Mus musculus GN=Tpt1 PE=1 SV=1	19450	38	2	1	8.1
VA0D1_MOUSE	Atp6v0d1	V-type proton ATPase subunit d 1 OS=Mus musculus GN=Atp6v0d1 PE=1 SV=2	40275	37	1	1	2.3
KCRB_MOUSE	Ckb	Creatine kinase B-type OS=Mus musculus GN=Ckb PE=1 SV=1	42686	37	1	1	5.5
EGLN_MOUSE	Eng	Endoglin OS=Mus musculus GN=Eng PE=1 SV=2	69976	37	1	1	1.5
EPHB2_MOUSE	Ephb2	Ephrin type-B receptor 2 OS=Mus musculus GN=Ephb2 PE=1 SV=3	109828	37	1	1	1.8
MATN4_MOUSE	Matn4	Matrikin-4 OS=Mus musculus GN=Matn4 PE=1 SV=1	68874	37	1	1	1.4

prot_acc	GN	prot_desc	prot_mass (Da)	prot_secre	Number of significant matches	Number of significant peptide sequences	Sequence coverage
MRP1_MOUSE	Abcc1	Multidrug resistance-associated protein 1 OS=Mus musculus GN=Abcc1 PE=1 SV=1	171075	36	1	1	0.6
CPNE2_MOUSE	Cpne2	Copine-2 OS=Mus musculus GN=Cpne2 PE=1 SV=1	60997	36	1	1	1.6
FBLN1_MOUSE	Fbln1	Fibulin-1 OS=Mus musculus GN=Fbln1 PE=1 SV=2	77981	36	1	1	1.7
AP2M1_MOUSE	Ap2ml	AP-2 complex subunit mu OS=Mus musculus GN=Ap2ml PE=1 SV=1	49623	35	1	1	1.8
FRMD8_MOUSE	Frmd8	FERM domain-containing protein 8 OS=Mus musculus GN=Frmd8 PE=1 SV=2	51795	35	1	1	6.7
MTPN_MOUSE	Mtpn	Myotrophin OS=Mus musculus GN=Mtpn PE=1 SV=2	12853	35	1	1	14.4
MYO9B_MOUSE	Myo9b	Unconventional myosin-IXb OS=Mus musculus GN=Myo9b PE=1 SV=2	238685	35	1	1	0.4
NPTN_MOUSE	Nptn	Neuroplastin OS=Mus musculus GN=Nptn PE=1 SV=3	44345	35	2	1	2.5
PSMD2_MOUSE	Psmd2	26S proteasome non-ATPase regulatory subunit 2 OS=Mus musculus GN=Psmd2 PE=1 SV=1	100139	35	1	1	0.9
RAC1_MOUSE	Rac1	Ras-related C3 botulinum toxin substrate 1 OS=Mus musculus GN=Racl PE=1 SV=1	21436	35	2	1	7.3
REXO1_MOUSE	Rexo1	RNA exonuclease 1 homolog OS=Mus musculus GN=Rexo1 PE=1 SV=1	130709	35	1	1	0.7
GPC5C_MOUSE	Gprc5c	G-protein coupled receptor family C group 5 member C OS=Mus musculus GN=Gprc5c PE=1 SV=2	48390	34	1	1	3
RL4_MOUSE	Rp14	60S ribosomal protein L4 OS=Mus musculus GN=Rp14 PE=1 SV=3	47124	34	1	1	1.9
SCRN1_MOUSE	Scrn1	Seecerin-1 OS=Mus musculus GN=Scrn1 PE=1 SV=1	46297	34	1	1	2.7
TAGL2_MOUSE	Tagln2	Transgelin-2 OS=Mus musculus GN=Tagln2 PE=1 SV=4	22381	34	1	1	5.5
AT1B3_MOUSE	Atp1b3	Sodium/potassium-transporting ATPase subunit beta-3 OS=Mus musculus GN=Atp1b3 PE=1 SV=1	31755	33	1	1	5
CAND1_MOUSE	Cand1	Cullin-associated NEDD8-dissociated protein 1 OS=Mus musculus GN=Cand1 PE=1 SV=2	136245	33	1	1	0.7
COSAI_MOUSE	Col5al	Collagen alpha-1(V) chain OS=Mus musculus GN=Col5al PE=1 SV=2	183564	33	1	1	0.5
PSB5_MOUSE	Psmb5	Proteasome subunit beta type-5 OS=Mus musculus GN=Psmb5 PE=1 SV=3	28514	33	1	1	3.4
RTN4_MOUSE	Rtn4	Reticulon-4 OS=Mus musculus GN=Rtn4 PE=1 SV=2	126535	33	1	1	1.1

prot_acc	GN	prot_desc	prot_mass (Da)	prot_secre	Number of significant matches	Number of significant peptide sequences	Sequence coverage
TFAM_MOUSE	Tfam	Transcription factor A, mitochondrial OS=Mus musculus GN=Tfam PE=1 SV=2	27970	33	1	1	2.9
TCPF_MOUSE	Cct5	T-complex protein 1 subunit epsilon OS=Mus musculus GN=Cct5 PE=1 SV=1	59586	32	1	1	3.1
DCTN2_MOUSE	Dctn2	Dynactin subunit 2 OS=Mus musculus GN=Dctn2 PE=1 SV=3	44090	32	1	1	4.7
GLOD4_MOUSE	Glo44	Glyoxalase domain-containing protein 4 OS=Mus musculus GN=Glo44 PE=1 SV=1	33296	32	1	1	3.4
S39AE_MOUSE	Slc39a14	Zinc transporter ZIP14 OS=Mus musculus GN=Slc39a14 PE=1 SV=1	53927	32	1	1	1.8
SODC_MOUSE	Sod1	Superoxide dismutase [Cu-Zn] OS=Mus musculus GN=Sod1 PE=1 SV=2	15933	32	1	1	7.8
UBPS5_MOUSE	Usp5	Ubiquitin carboxyl-terminal hydrolase 5 OS=Mus musculus GN=Usp5 PE=1 SV=1	95772	31	1	1	1

Abbreviations used for protein and peptide identification summary tables

prot_acc: Accession number according to protein family or pyrosequencing coread

GN: Gene name

prot_desc: Description

prot_mass: Molecular weight of translated sequence